



Deep Yedoma permafrost: A synthesis of depositional characteristics and carbon vulnerability



Jens Strauss^{a,*}, Lutz Schirrmeister^a, Guido Grosse^{a,b}, Daniel Fortier^c, Gustaf Hugelius^d, Christian Knoblauch^e, Vladimir Romanovsky^f, Christina Schädel^g, Thomas Schneider von Deimling^h, Edward A.G. Schuur^g, Denis Shmelevⁱ, Mathias Ulrich^j, Alexandra Veremeevaⁱ

^a Alfred Wegener Institute Helmholtz Centre for Polar and Marine Research, Periglacial Research Unit, Potsdam, Germany

^b University of Potsdam, Institute of Earth and Environmental Sciences, Potsdam, Germany

^c Université de Montréal, Département de Géographie, Montréal, Canada

^d Stockholm University, Department of Physical Geography, Stockholm, Sweden

^e Universität Hamburg, Institute of Soil Science, Hamburg, Germany

^f University of Alaska Fairbanks, Geophysical Institute, Fairbanks, USA

^g Northern Arizona University, Center for Ecosystem Science and Society, Flagstaff, USA

^h Max Planck Institute for Meteorology, Hamburg, Germany

ⁱ Institute of Physicochemical and Biological Problems in Soil Science, Russian Academy of Sciences, Pushchino, Russia

^j Leipzig University, Institute for Geography, Leipzig, Germany

ARTICLE INFO

Keywords:

Perennial frozen ground
Thermokarst
Arctic
Late Pleistocene
Greenhouse gas source
Climate feedback

ABSTRACT

Permafrost is a distinct feature of the terrestrial Arctic and is vulnerable to climate warming. Permafrost degrades in different ways, including deepening of a seasonally unfrozen surface and localized but rapid development of deep thaw features. Pleistocene ice-rich permafrost with syngenetic ice-wedges, termed Yedoma deposits, are widespread in Siberia, Alaska, and Yukon, Canada and may be especially prone to rapid-thaw processes. Freeze-locked organic matter in such deposits can be re-mobilized on short time-scales and contribute to a carbon-cycle climate feedback. Here we synthesize the characteristics and vulnerability of Yedoma deposits by synthesizing studies on the Yedoma origin and the associated organic carbon pool. We suggest that Yedoma deposits accumulated under periglacial weathering, transport, and deposition dynamics in non-glaciated regions during the late Pleistocene until the beginning of late glacial warming. The deposits formed due to a combination of aeolian, colluvial, nival, and alluvial deposition and simultaneous ground ice accumulation. We found up to 130 gigatons organic carbon in Yedoma, parts of which are well-preserved and available for fast decomposition after thaw. Based on incubation experiments, up to 10% of the Yedoma carbon is considered especially decomposable and may be released upon thaw. The substantial amount of ground ice in Yedoma makes it highly vulnerable to disturbances such as thermokarst and thermo-erosion processes. Mobilization of permafrost carbon is expected to increase under future climate warming. Our synthesis results underline the need of accounting for Yedoma carbon stocks in next generation Earth-System-Models for a more complete representation of the permafrost-carbon feedback.

1. Introduction

1.1. Long-term permafrost dynamics

Permafrost is a characteristic feature of the circum-Arctic region that is not covered by ice sheets and glaciers. It occurs in regions characterized by cold winter temperatures, in combination with low

snow depth, that result in a long-term negative annual heat energy balance of the land surface. Today, the permafrost region in the Northern Hemisphere covers approximately 23 million km² or ~24% of the terrestrial area (Brown et al., 1998).

Similar to warming from the late Pleistocene to Holocene when permafrost retreated from the last permafrost maximum to today's extent, future warming may result in deeper thaw in these regions and

* Corresponding author at: Alfred Wegener Institute Helmholtz Centre for Polar and Marine Research, Periglacial Research Unit, Potsdam, Telegrafenberg A43, DE-14471 Potsdam, Germany.

E-mail address: Jens.Strauss@awi.de (J. Strauss).

<http://dx.doi.org/10.1016/j.earscirev.2017.07.007>

Received 1 February 2017; Received in revised form 13 July 2017; Accepted 14 July 2017

Available online 24 July 2017

0012-8252/ © 2017 The Authors. Published by Elsevier B.V. This is an open access article under the CC BY-NC-ND license (<http://creativecommons.org/licenses/by-nc-nd/4.0/>).

further massive reduction of permafrost extent. The long-term impact of climatic change on permafrost can be best understood when comparing past with modern permafrost extent. Maximum cold-climate conditions during the Last Glacial Maximum resulted in a maximum permafrost extent for the last glacial-interglacial cycle (Lindgren et al., 2015). The circum-Arctic permafrost extent during this period was approximately 35 million km², or about ~52% larger than today (Lindgren et al., 2015). We focus on the characteristics and dynamics of ice-rich permafrost deposits containing large syngenetic (freezing shortly after deposition) ice wedges, called Yedoma deposits, which accumulated in vast unglaciated regions of Eurasia, Alaska, and Northwest Canada during the Pleistocene (Schirmer et al., 2013). The unglaciated regions of Eurasia, Alaska, and Northwest Canadian lowlands were favourable for Yedoma deposition because here an extreme continental climate combined with a low topographic gradient caused steady conditions for polygonal ice wedge growth with ongoing sedimentation by water and wind. Yedoma deposits are ancient deposits and there is no known recent accumulation. Today, the Yedoma domain still covers > 1 million km² of the northern permafrost zone (Grosse et al., 2011b). There are two key differences between Yedoma deposits and other permafrost deposits: (1) the ground ice properties of these deposits, and (2) their large spatial extent and thicknesses, causing a large total volume. These characteristics make Yedoma highly vulnerable to rapid thaw, induced by climate warming, which becomes significant, because of re-mobilization of organic carbon that has been sequestered for millennia. Here we use the term Yedoma domain, which includes the Yedoma deposits itself and frozen deposits that accumulated after Yedoma degradation in thermokarst landforms (Olefeldt et al., 2016).

Concerning the organic carbon quantity, the permafrost region in general has been characterized as ‘Pandora’s freezer’ (Brown, 2013), and its potential to act as a ‘carbon bomb’ in the climate system was discussed (Treat and Frolking, 2013). Yedoma deposits in particular were targeted as a ‘sleeping giant’ in the carbon cycle (Mascarelli, 2009). Although it may fall outside the usual scientific language, these characterizations well describe the current level of uncertainty surrounding our understanding of a carbon pool of significant size in a vulnerable region of the Earth System (Fig. 1). Recently, the Yedoma domain has been discussed as one of the potential climate tipping elements (Lenton, 2012).

Permafrost may degrade in different ways, depending on climatic and ecological conditions as well as permafrost characteristics such as ground temperature and ground ice content. The major processes are

(a) ground warming and increase in unfrozen water content (Kurylyk et al., 2016), (b) top-down thaw by long-term thickening of the surface layer on top of permafrost that is subject to seasonal thawing and freezing (active layer) (Hinkel and Nelson, 2003), (c) thermo-erosion along coasts, rivers, and lake shores (Günther et al., 2013; Jones et al., 2011; Kanevskiy et al., 2016) and (d) rapid thaw induced by thermokarst and thermoerosional processes in lowlands, wetlands, and hillslopes. Thermokarst and talik (a volume of perennially unfrozen ground above or inside permafrost) formation, caused by basin development with melting of excess ground ice (ice exceeding the sediment pore volume) and draining of melt water, can result in deep thaw and surface subsidence. Ice-rich permafrost, like Yedoma deposits, is especially prone to these processes, and thaw subsidence of up to 30 m has been described for example in Northeast Siberia (Ulrich et al., 2014).

Observations and forecast models suggest further warming and thawing of permafrost in many regions in the coming centuries (Romanovsky et al., 2010) and highlight the potential for additional significant release of old organic carbon, which would contribute to a transfer of long-term sequestered carbon to the atmosphere, a process considered irreversible on human timescales (Koven et al., 2015; Schaefer et al., 2011; Schuur et al., 2015). Following modelling studies, a large contribution of permafrost carbon to glacial-interglacial CO₂ changes showed that the permafrost carbon feedback can be large (Köhler et al., 2014). Thus, although permafrost deposits with their large carbon stocks are located in one of the world’s most remote regions, considering these thawing deposits in the context of the global carbon cycle and climate change is of utmost importance.

1.2. Aims and objectives

To better understand how the Yedoma domain will respond to the warming climate and may contribute to global climate change, it is essential to synthesize current knowledge on Yedoma deposits. Of particular interest is their genesis, as the original depositional environments determine many parameters relevant for vulnerability of these deposits to thaw and carbon mobilization, including organic matter (OM) source, age, state of decomposition, and quantity, as well as ground-ice distribution, and the thickness of accumulated sediment as well as the possible maximum depths reached by thaw in the past. Our objectives for this synthesis are therefore to (a) summarize and evaluate existing hypotheses on Yedoma genesis, to (b) provide an overview of the age of deposits and organic carbon stored in Yedoma, and to (c) evaluate datasets on Yedoma carbon quantity and quality that allow conclusions on the vulnerability of this organic carbon pool.

2. Permafrost carbon: a large dormant organic carbon pool under climate pressure

Circum-Arctic ecosystems, including the permafrost region, have strong feedbacks to the Earth’s climate system. By cooling the Earth through reflecting sunlight directly due to high albedo and sequestering atmospheric carbon in cold and wet soils and frozen sediments, circum-Arctic regions function like a global air conditioner (Euskirchen et al., 2013). However, surface air temperatures in polar regions are rising about twice as fast as the global mean (Overland et al., 2015). This rapid warming trajectory increases the frequency, and magnitude of disturbances in the permafrost region (Grosse et al., 2011a). Resulting permafrost thaw will re-introduce organic carbon into the carbon cycle via OM decomposition, which increases the amount of the greenhouse gases carbon dioxide (CO₂) and methane (CH₄) flux to the atmosphere and causes a positive feedback to global warming. This feedback loop (Fig. 2) would represent a substantial carbon-climate feedback mechanism, but it is less well quantified than many other climate feedback processes. Recent syntheses using incubation studies have quantified OM decomposition rates (Schädel et al., 2014) and greenhouse gas production potentials (e.g. CO₂:CH₄ ratio in released carbon) for

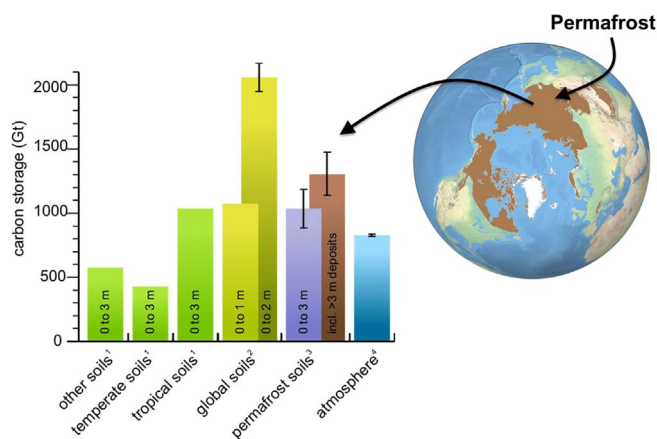


Fig. 1. Global carbon storage in soils and atmospheric carbon. Inventories from ¹Jobbágy and Jackson (2000); other soils includes carbon stored in croplands, deserts and clerophyllous shrublands, ²Köchy et al. (2015) for the 0 to 1 m estimate, Batjes (2016) for the 0 to 2 m, ³Hugelius et al. (2014); Strauss et al. (2013) and ⁴Ciais et al. (2013). The permafrost distribution follows Brown et al. (1998). Error bars are included if available in the cited studies. (For interpretation of the references to colour in this figure legend, the reader is referred to the web version of this article.)

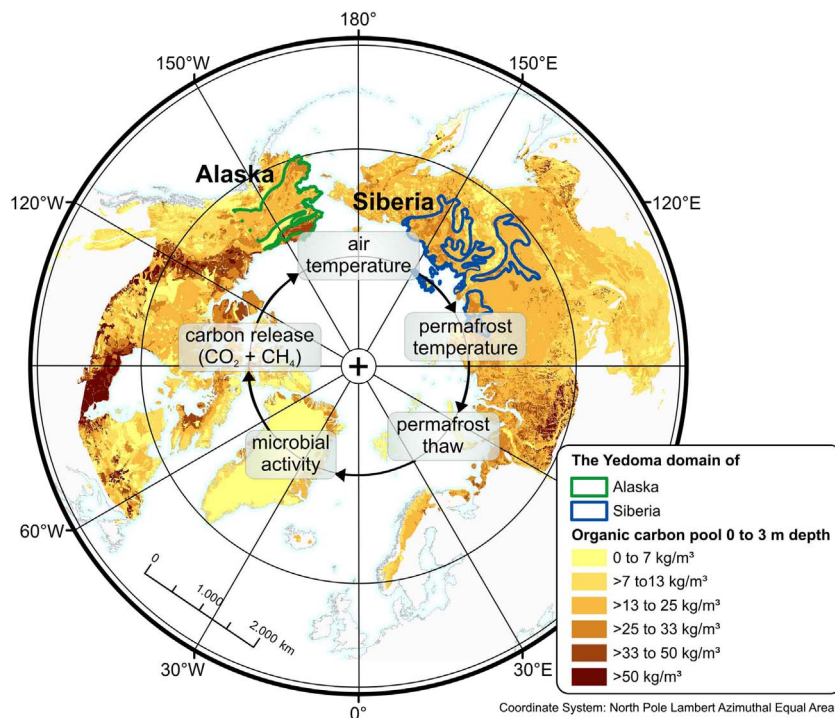


Fig. 2. Map of estimated 0 to 3 m deep carbon inventory stored in the circum-Arctic permafrost region (Hugelius et al., 2014; Kanevskiy et al., 2011; Romanovskii, 1993). The eastern boundary of Canadian Yedoma areas is uncertain, indicated as a dotted line at the Alaskan/Yukon state border. The conceptual permafrost carbon climate feedback cycle is illustrated in the middle. The Yedoma domain marks the potential maximum occurrence of widespread Yedoma deposits but also includes other deposits that formed after degradation of Yedoma, such as thermokarst deposits. In West Siberia and the Russian Far East Yedoma occurs sporadically, e.g. in river valleys.

permafrost under aerobic and anaerobic incubation conditions. Despite these recent efforts, there is still a large uncertainty associated with permafrost OM decomposition.

Besides the near-surface carbon stored in permafrost (Zubrzycki et al., 2014), thermokarst degradation processes may rapidly mobilize deeper permafrost carbon ('deep' is used here to describe carbon deeper than the modern active layer). While OM input in these soils is low compared to surface soils, cold and waterlogged conditions substantially slow down OM decomposition, and once soils become perennially frozen, it mostly ceases. Continued accumulation, cryoturbation, and freezing over millennia essentially result in the disconnection of permafrost OM from the surface carbon turnover. The frozen deep organic carbon is thus often many thousands of years older than the surface organic carbon. The favourable preservation conditions are a unique feature to permafrost environments and lasted for tens of millennia in many unglaciated circum-Arctic regions. Of particular interest in a warming climate are the permafrost areas that are rich in ground ice (> 20% ice content (Brown et al., 1998)), which cover about 8.8% of the total circum-Arctic permafrost region (Brown et al., 1998). Here, the large amount of ice increases the vulnerability of permafrost deposits to disturbances (Grosse et al., 2011a), since rapid surface subsidence may occur if the excess ice thaws. Thus, ground ice is a key factor in assessing the vulnerability of the landscape and permafrost-stored organic carbon. Though all permafrost types can be affected by thawing, degradation of thick ice-rich permafrost deposits containing a large carbon pool may cause particularly strong feedbacks to permafrost ecosystems by significantly changing topography and hydrology. One of these feedbacks is abrupt thaw after thermokarst lake formation, including dramatically speed up in thaw rates once the lakes are deep enough to prevent winter-refreeze. This alters the carbon cycle by releasing substantial amounts of carbon previously frozen for millennia (Schuur et al., 2008). Recent estimates of carbon stocks in permafrost quantify 472 ± 27 Gt for the upper 1 m of soils and 1035 ± 150 Gt for the depth from 0 to 3 m (Hugelius et al., 2014) (Fig. S1). Several studies attributed a considerable carbon stock of several 100's of Gt of organic carbon to the frozen deep deposits in Arctic deltas and in the Yedoma domain, comparable in size with the entire carbon pool in the upper 1 m (Hugelius et al., 2014; McGuire et al., 2010; Schuur et al.,

2015; Strauss et al., 2013; Walter Anthony et al., 2014; Zimov et al., 2006). Hence, this deep but still thaw-vulnerable pool needs special consideration in carbon cycle studies.

The fate of the organic carbon stored in thawing permafrost depends on various factors controlling OM decomposition, e.g. OM quality and stabilization, temperature, hydrology, microbial communities, vertical and lateral distributions of carbon stocks and time. Some permafrost affected landscapes still act as a carbon sink (Kutzbach et al., 2007; van der Molen et al., 2007; van Huissteden and Dolman, 2012; Walter Anthony et al., 2014), while others are carbon sources (Hayes et al., 2011; Natali et al., 2014). However, once unlocked by thaw, permafrost OM is prone to microbial decomposition resulting in the production of CO₂ and CH₄ (Dutta et al., 2006; Mackelprang et al., 2011; Schuur et al., 2009). While processes like carbon sequestration by vegetation act in the opposite direction and may temporarily increase the carbon sink capacity of the northern high latitudes (McGuire et al., 2010; van Huissteden and Dolman, 2012), thaw and release of deep organic carbon from Yedoma deposits that has been sequestered over most of the last glacial period may exceed such sinks and act as a strong carbon source.

3. Study region and general characteristics of Yedoma deposits

Major parts of the northern hemisphere remained unglaciated during the last ice age and became permafrost-dominated (Lindgren et al., 2015). Because of a lower sea level, major shelf areas of the Arctic Ocean were not submerged and thus an interconnected landmass existed between the Scandinavian and Laurentide ice sheets. Together with the unglaciated portions of eastern Siberia as well as Alaska and westernmost Northwest Canada this region is termed Beringia. Long-term continuous sedimentation and syngenetic freezing into permafrost during the late Pleistocene resulted in accumulation of thick periglacial deposits. Moreover, steady polygonal ice-wedge growth with ongoing sedimentation such that massive syngenetic ice wedges formed a significant component is a key characteristic of the Yedoma deposits itself (Kanevskiy et al., 2011). The largely ice-rich silt and fine sand deposits still cover extensive lowlands and hillslopes in the Beringian region (Kaplina et al., 1978; Péwé, 1975; Péwé and Journaux, 1983; Sher,

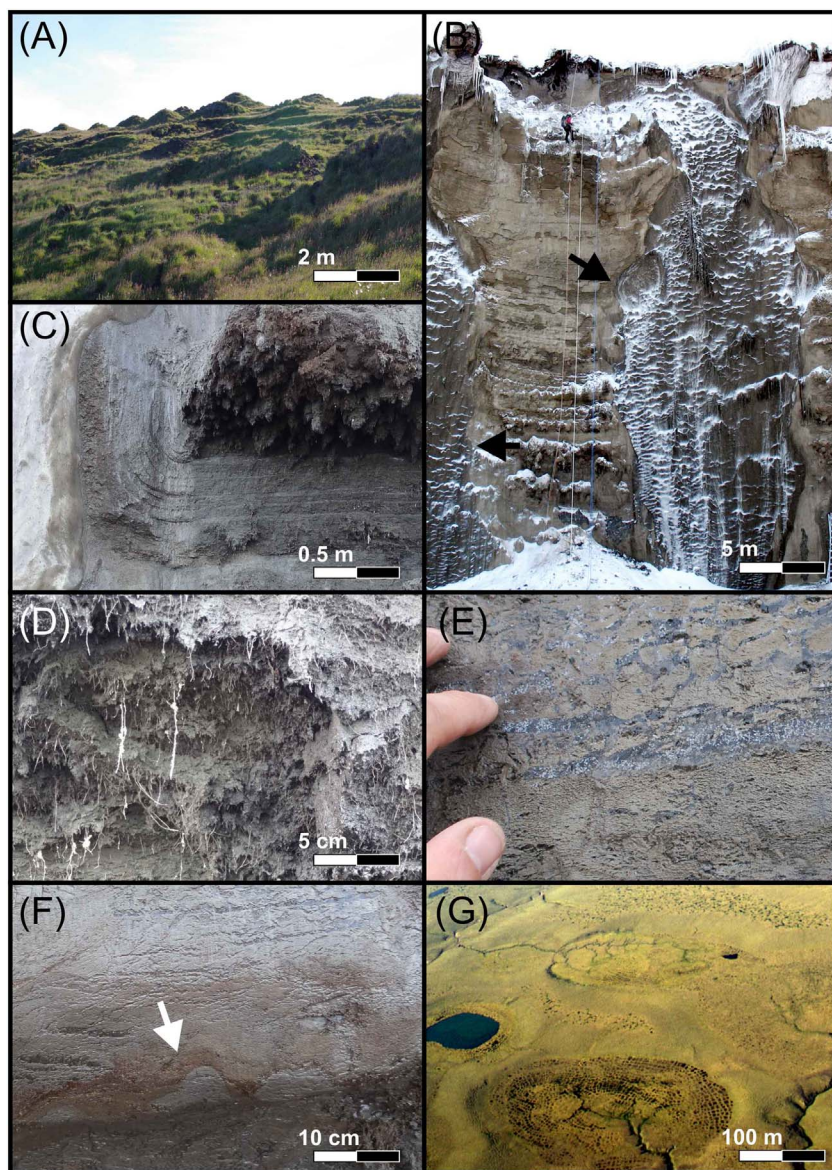


Fig. 3. Typical phenomena of Yedoma deposits and Yedoma landscapes. (A) conical thermokarst mounds (called baidzharakhs in Russia) that developed from sediment-rich polygon centres and the thawing of surrounding large syngenetic ice wedges (Buor Khaya Peninsula, Siberia, 2010) (B) Yedoma bluff, eroded by the Itkillik River (Alaska, 2012). The presence of ice-wedge shoulders (arrows) indicate the position of the paleo active layer and episodic sedimentation of the sediments on the polygonal ground surface; (C) peat layer and vertically-deformed sediments and ice bands along a syngenetic ice-wedge on Sobo-Sise Island (Lena Delta, Siberia, 2014); (D) late Pleistocene plant remains (grass roots) in Yedoma deposits on Sobo-Sise Island (2014); (E) typical cryostructures in Yedoma deposits, here irregular reticulate in the upper part, one ice band in the middle and wavy lenticular in the lower part (photo by D. Fortier, 2012 at Itkillik River exposure, Alaska); (F) cryoturbated fine dispersed organic carbon (white arrow) on Sobo-Sise Island (2014); (G) aerial view of a Yedoma landscape affected by thermokarst degradation at Cape Svyatoy Nos (Laptev Sea, Siberia, 1999), including Yedoma hills and thermokarst depressions with lakes and (partly) drained lake basins.

Photo credits: A–F: J. Strauss; G: L. Schirrmeister.

1971; Sher, 1997) (Figs. 2, 3G).

Due to incorporation of OM into permafrost from active layer, Yedoma deposits can contain well-preserved OM (Dutta et al., 2006; Strauss et al., 2015). The relatively constant sedimentation and large syngenetic ice content in Yedoma deposits also resulted in a great depositional thickness of up to 50 m (Kanevskiy et al., 2011; Schirrmeister et al., 2013) (Fig. 3B). Adding the recent maximum Yedoma domain of 1.4 million km² (Fig. 2) and postulating that Yedoma deposits occupied 80% (Walter et al., 2007) of the adjacent formerly exposed and now flooded Arctic shelves (1.9 million km², down to 120 m below modern sea level, between 105°E – 128°W and > 68°N) (Brosius et al., 2012), the maximum extent of the Yedoma domain is estimated to be at least 3.3 million km² during the Last Glacial Maximum. Beyond this, similar deposits may have existed in formerly periglacial regions where permafrost has disappeared, such as in central Europe, the Russian Plain, or the North American Plains like the Great Plains. In addition to the original and still intact Yedoma deposits, the Yedoma domain comprises other stratigraphic types of deposits (Fig. S2). Yedoma degradation has occurred due to postglacial warming especially during the deglacial and the early Holocene (Kanevskiy et al., 2014; Morgenstern et al., 2013), and an important suite of deposits is associated with thermokarst landforms. Sediments in thermokarst depressions are

composed of reworked Yedoma deposits as well as Holocene accumulation during sub-aquatic and sub-aerial phases.

4. Yedoma origin: how did Yedoma deposits accumulate?

The overarching similarities of Yedoma deposits in different regions are their composition of ice-rich fine-grained sediments (Schirrmeister et al., 2011b; Strauss et al., 2013), the presence of large syngenetic ice wedges (Kanevskiy et al., 2011; Ulrich et al., 2014), unique cryostructures including dense reticulated ice lenses and horizontal ice bands (Kanevskiy et al., 2011), and fossils remains of the late Pleistocene mammoth mega-fauna, insects and tundra-steppe flora (Andreev et al., 2009; Kuzmina et al., 2011). The late Pleistocene vegetation is the main source of OM sequestered in Yedoma deposits, and their origin, biogeochemical composition, and state of preservation determine the OM vulnerability. Yedoma deposits started accumulating during the last ice age. No older Yedoma deposits older than the last interglacial (MIS-5e; 130–115 thousand yrs BP) are described so far (Schirrmeister et al., 2013). We suppose that Yedoma deposits degraded during former warmer-than-Holocene (e.g. Turney and Jones, 2010) interglacial periods. While in several locations radiocarbon ages of the Yedoma base are beyond the ¹⁴C dating range, optically and thermally stimulated

luminescence dates and extrapolation of continuous sedimentation rates to basal units of the Yedoma indicate a starting period for the oldest locations during stadial conditions in marine isotope stage (MIS) 4 (71–60 thousand yrs BP) (Schirrneister et al., 2011b). In other locations, Yedoma accumulation started much later during the interstadial MIS 3 (60–24 thousand yrs BP, Schirrneister et al., 2011b). To cover the depositional period and to examine the end of Yedoma accumulation, we compiled the largest available database of radiocarbon ages from Yedoma deposits from > 50 individual sites. A range of in situ materials have been dated ranging from plant macrofossils and animal remains to bulk sediments. Though there is a large body of literature on the mammoth fauna complex (e.g. Zimov et al., 2012) that accompanied the Yedoma accumulation environment and several syntheses have been compiled on mammal bone and soft tissue ages falling within the Yedoma accumulation period (Schirrneister et al., 2002), we here only include dates of in situ animal remains found in the Yedoma deposits. Most of the original dates have been acquired for the purpose of paleo-environmental reconstruction and stratigraphical assessments, some to allow assessments of sediment accumulation rates, and others to provide context for carbon cycle, microbiological, paleontological, or paleogenetic studies. The bulk of dating has been done for sites in Siberia (619 dates), with minor contributions in the database coming from Alaska (75 dates) and NW Canada (19 dates). Yedoma accumulation ended in most places abruptly at the late Pleistocene – Holocene transition (Fig. 4), when thermokarst processes rapidly began re-configuring local hydrology and deposition/erosion patterns (e.g. Walter et al., 2007). In several locations, the youngest (MIS 2, 24–11 thousand yrs BP) horizons of the Yedoma were eroded, resulting in stratigraphic gaps of several thousand years (Schirrneister et al., 2011b).

There are several different viewpoints on Yedoma genesis (Table S2) (Murton et al., 2015; Strauss et al., 2012), and there is a broad consensus (Hubberten et al., 2004; Schirrneister et al., 2013; Sher, 1995) that neither glacier-related sedimentation, nor shallow-marine sedimentation were involved. Researchers working in the Yukon area and Alaska often characterize Yedoma silts as loess or re-transported loess (Péwé, 1955; Sanborn et al., 2006). Researchers working in Siberia have proposed several different hypotheses (Schirrneister et al., 2011b) about the sedimentation regime of Yedoma. In general, integrating the hypotheses of Table S2, the polygenetic hypothesis with a distinct aeolian input is the most popular in the recent scientific literature (Schirrneister et al., 2013). In our point of view, if the re-transportation of loess (also called secondary loess) is included in the loess concept (Murton et al., 2015; Péwé and Journaux, 1983; Tomirdiario, 1980;

Tomirdiario and Chernen'kiy, 1987), the loess and the polygenetic concepts could be merged.

Yedoma deposits are described as ice-saturated or supersaturated silts and fine sands with segregation ice contents representing ~30 to 40 vol% of the frozen material in addition to syngenetic ice wedges (Strauss et al., 2013). Using different geomorphometric mapping methods similar ice contents between 44 vol% and 48 vol% were found for Yedoma deposits (Günther et al., 2015; Ulrich et al., 2014). Thus, the total volume of Yedoma deposits is composed of ~80 vol% ground ice (Kanevskiy et al., 2011; Strauss et al., 2013), making ice the major structural component. This differs from previous characterizations of classical loess, where coarse silt to fine sand is the dominating component of the deposit (Pécsi, 1990).

Even removal of the ice component upon thaw would not result in a deposit with the structural properties of pure loess, as the loss of 80 vol % ground ice, subsidence, and erosion would fundamentally alter the sedimentary structure and stratigraphy of the deposit. Poorly sorted bito multi-modal grain-size distribution (Schirrneister et al., 2013; Strauss et al., 2012) point to a variety of depositional mechanism, but could be also the signal of aeolian deposition (Sun et al., 2004). Synthesizing this, a variety of re-transport processes and likely seasonal differentiation (Strauss et al., 2012), intensified by cryogenic weathering of quartz grains during seasonal freeze-thaw cycles in the active layer, are involved in Yedoma accumulation. Thus, we propose that Yedoma deposits have a polygenetic origin with a variety of processes contributing to their formation under sustained cold-climatic, periglacial environmental conditions. Including regional differences the major processes are aeolian deposition, water-related (such as floodplain overbank deposition or alluvial runoff and slope processes), cryogenic weathering and syngenetic ground ice accumulation (Fig. S3). This synthesizing hypothesis also considers two general formation processes that are lacking in other hypotheses: (a) Primary accumulation of sediments in low-centred ice-wedge polygons, and (b) the synchronous freezing of deposits being accompanied by ice-wedge growth.

Proposing a availability of fine grained source material likely derived from cryogenic weathering, fluvial, lacustrine, or pre-existing aeolian sediments and not much stabilizing sparse vegetation, a possible scenario of Yedoma accumulation includes (1) the flooding of alluvial areas after snowmelt and during periods of high river discharge, and (2) aeolian deposition occurring in dry seasons (Strauss et al., 2012) or when parts of the formerly submerged floodplain areas become susceptible to wind activity (Muhs and Bettis, 2003). Local source of fine grained material may serve to produce both aeolian deposition and/or alluvial deposits, and result in a similar mineralogy

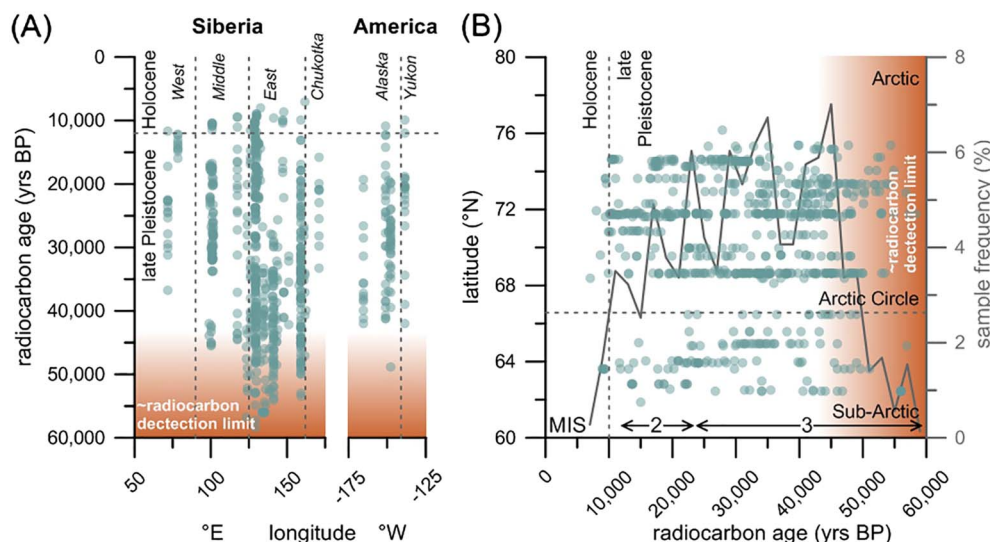


Fig. 4. Spatial distribution of radiocarbon ages of Yedoma deposits. A: radiocarbon ages versus geographical longitude of study site. A range of in situ materials have been dated ranging from plant macrofossils (peat, roots, seeds, moss, grass, woody materials, plant detritus, etc.) and animal remains (insects, mammal bones, bone collagen, and tissue, excrements) to bulk material (paleosols, sediments); B: radiocarbon ages versus geographical latitude of study site. ¹⁴C dates were compiled from different sources given with locations in Table S1. The grey frequency line illustrates the relative sample frequency in each age class (2000 yrs per class, 27 classes). The brown shading visualizes the radiocarbon detection limit, incl. minimal ages (beyond the detection limit). The Marine Isotope Stage (MIS) classes are labelled at the bottom. (For interpretation of the references to colour in this figure legend, the reader is referred to the web version of this article.)

throughout the Yedoma deposit, as observed in Siberia (Fig. S4) in a well-studied Yedoma deposit (Strauss et al., 2015). This concept of Yedoma genesis, while allowing different sediment facies types, builds on comparable environmental conditions for regions where Yedoma could accumulate: Lowland to rolling foothill landscape dominated by ice wedge polygonal networks, stable relief characteristics with poorly-drained accumulation areas, harsh continental, cold-arid climate conditions causing sparse vegetation cover, presence of intense periglacial weathering processes, and the occurrence of nearby sediment sources such as low mountain ranges (Fig. S3). In eastern Beringia, the aeolian component appears to be more pronounced (Froese et al., 2009; Péwé, 1975) than in most regions of western Beringia, but the variety of contributing processes are similar.

5. Yedoma domain organic carbon

5.1. Inventories: how much organic carbon is stored in the Yedoma domain?

A sparse number of studies and available data so far prevent a full understanding of the Yedoma domain for global carbon cycling. Several recent studies and reviews (Grosse et al., 2013; Hugelius et al., 2014; Koven et al., 2015; Schirrmeister et al., 2013; Schuur et al., 2015; Strauss et al., 2013; Walter Anthony et al., 2014) provide solid progress towards a better quantification of the permafrost carbon pool size.

Major subsurface carbon inventories in the Yedoma domain include (a) the Yedoma deposits, (b) thermokarst deposits, (c) taberal deposits, (d) the active layer, as well as (e) dissolved organic carbon in ground ice. We use the term taberal by generalizing the definition of taberal deposits (also called taberite) by Kaplina (1981) in the sense of the process of in-situ thawing Yedoma under a large water body. Independently from the recent ground temperature (refrozen or non-frozen), taberal deposits here are included as former Yedoma sediments that underwent thawing in a talik, resulting in diagenetic alteration of sediment structures (i.e., loss of original cryostructure, sediment compaction) and biogeochemical characteristics. Different approaches have been used in previous studies to calculate the Yedoma domain carbon inventory. A first attempt to estimate a total Yedoma carbon pool (Zimov et al., 2006) was based on a mean deposit thickness of 25 m, 1,000,000 km² areal coverage, 2.6 wt% total organic carbon (TOC), a bulk density (BD) of 1.65 10³kg/m³, and 50 vol% wedge-ice volume, resulting in 450 Gt organic carbon. Based on new lower bulk density data (0.89 to 0.96 10³kg/m³), this pool was suggested to be reduced by 25 to 50% (Schirrmeister et al., 2011a), resulting in a pool of ~225 to 338 Gt carbon. A recent study (Walter Anthony et al., 2014) calculated a total Pleistocene-carbon pool size of 284 ± 40 Gt for the Yedoma domain as the sum of Pleistocene carbon in (a) undisturbed Yedoma (129 ± 30 Gt), (b) Yedoma thawed in taliks underneath thermokarst lakes (114 Gt), taberal deposits, defined in Schneider von Deimling et al. (2015), and (c) thermokarst basins where portions of the Pleistocene carbon has been reworked in thermokarst deposits (41 Gt). By adding Holocene carbon stored in soil formed on top of Yedoma deposits (13 ± 1 Gt) and as peaty and organic-rich lacustrine and palustrine sediments in thermokarst basins (159 ± 24 Gt), the Yedoma domain inventory was estimated to contain 456 ± 45 Gt carbon, including thawed deposits (Fig. 5) (Walter Anthony et al., 2014).

Given the skewness of the carbon content data distribution, a statistically more robust approach to calculate carbon inventory incorporates bootstrapped mean values rather than arithmetic means for the statistical analysis and upscaling (Strauss et al., 2013). Using this method, the calculated Yedoma domain inventory is 83 ± 60 Gt organic carbon for Yedoma deposits and 128 ± 98 Gt organic carbon for thermokarst deposits, for a total of 211 ± 158 Gt organic carbon for the entire Yedoma domain, not considering taberal deposits. To reduce the high uncertainty of the calculations, an adjusted bootstrapping algorithm was used (Hugelius et al., 2014). The estimates are 83 ± 12 Gt for Yedoma deposit carbon and 130 ± 29 Gt for

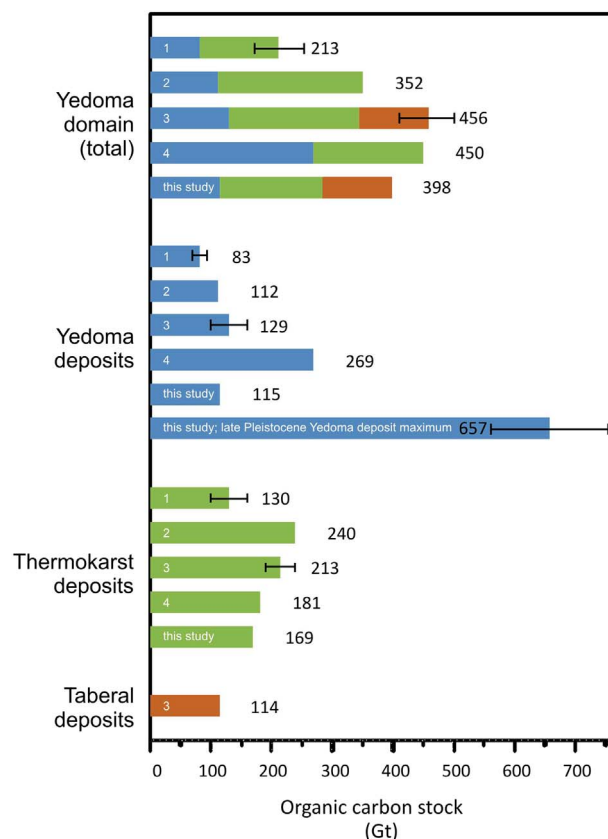


Fig. 5. Comparison of the different carbon stock calculations from the Yedoma domain. The superscript numbers are related to the publications: 1: Strauss et al. (2013) (bootstrapping approach); 2: Strauss et al. (2013) (simple-mean approach); 3: Walter Anthony et al. (2014), 4: Zimov et al. (2006) and 'this study' best average using the minimum (Strauss et al., 2013) and maximum calculations (Walter Anthony et al., 2014). Here, combining the uncertainty estimation was not possible as the numbers were calculated differently (interquartile range and standard deviation). The colours are used to highlight the different stocks. Yedoma deposits are illustrated in blue, thermokarst deposits in greenish and taberal deposits orange colour. We merged some pools published Walter Anthony et al. (2014): we added the Holocene carbon (159 ± 24, and 13 ± 1 Gt) and reworked Pleistocene carbon (41 Gt) stored in Holocene thermokarst landforms, resulting into a total of 213 ± 25 Gt for the thermokarst deposit carbon pool. Error bars are included if available in the cited studies. (For interpretation of the references to colour in this figure legend, the reader is referred to the web version of this article.)

thermokarst deposits. Based on this calculation 213 ± 41 Gt organic carbon are stored in the Yedoma domain (Fig. 5), also not considering taberal deposits. Of this pool, approximately 32 Gt organic carbon are stored in the first ~1 to 3 m (assuming an active layer down to 1 m) (Hugelius et al., 2014) (Figs. 6, 7).

For the mean-based calculation approach, the proportions between Yedoma deposits and thermokarst deposits are also similar (Strauss et al., 2013; Walter Anthony et al., 2014; Zimov et al., 2006) (Fig. 5). Adding the Yedoma-derived taberal deposits (114 Gt organic carbon) and not considering the bootstrap-adjusted method, the lower Yedoma domain estimate (Strauss et al., 2013) would yield a Yedoma domain carbon pool of 466 Gt, which is similar to the other calculations (Walter Anthony et al., 2014; Zimov et al., 2006) (Fig. 5). More organic carbon was estimated in thermokarst deposits compared to the original Yedoma deposits (Strauss et al., 2013; Walter Anthony et al., 2014), suggesting that thermokarst lakes and basins acted as a long-term carbon sink over the Holocene by partially burying Pleistocene carbon and sequestering Holocene carbon in wetlands, hydric soils, peat and lake sediments. This also means that their currently large carbon pool, much of it frozen during the Holocene, may have a large climate impact if thawing caused by a continued warming will re-mobilize portions of this pool. But up to now, if Yedoma thaws forming thermokarst, more

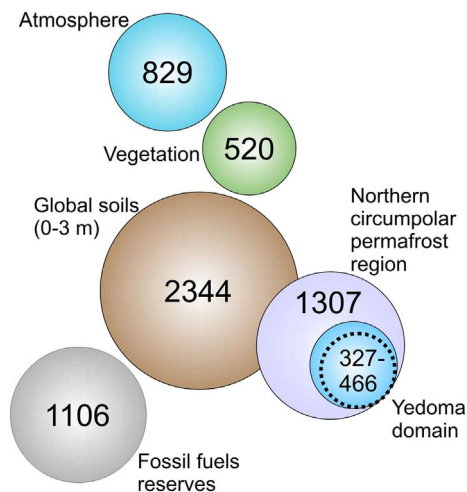


Fig. 6. Terrestrial carbon stock and atmospheric carbon in relation to the carbon stored in the Yedoma domain. The surface area of the circles represents the size of the carbon stock. The stocks are given in Gt. The global soils estimate is published by Jobbágy and Jackson (2000). For atmosphere, vegetation, and fossil fuels, means are taken of the minimum - maximum ranges from Ciais et al. (2013). The circum-Arctic permafrost region as well as the surface pools and the permafrost terrain carbon are calculated by Hugelius et al. (2014). The Yedoma domain carbon inventories are taken from Strauss et al. (2013) and Walter Anthony et al. (2014). The dotted circle represents the lower range of the estimates for the Yedoma domain. Details for the 1307 Gt of the northern circumpolar permafrost region are shown in Fig. 7.

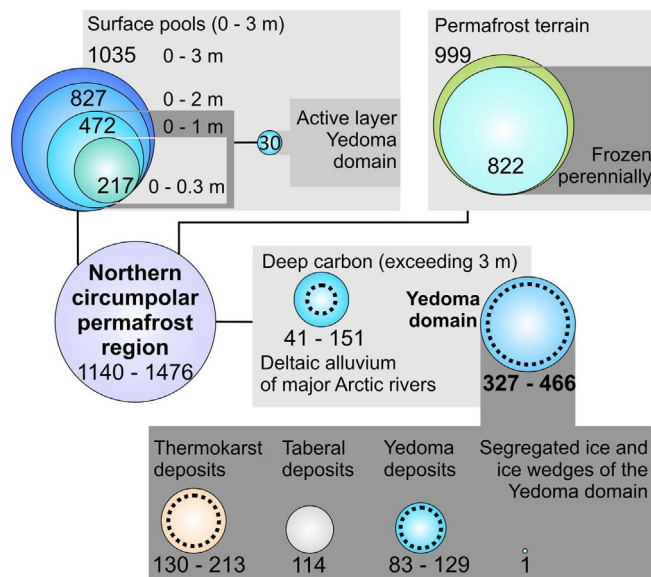


Fig. 7. Carbon stock of the Yedoma domain and the northern circumpolar permafrost. The circum-Arctic permafrost region (excluding exposed bedrock, glaciers and ice-sheets and water bodies, but including the full areal extent of regions where permafrost coverage is discontinuous so that a significant fraction of the area is not in permafrost terrain) as well as the surface pools and the permafrost terrain carbon are calculated in Hugelius et al. (2014). Permafrost terrain includes carbon storage Arctic soils and in permafrost in Yedoma or permafrost deltaic deposits below 3 m depth. Deltaic alluvium below 3 m was published as 91 ± 52 Gt (Hugelius et al., 2014). Here we included the -0.5 m (assumed active layer 0.5 m) to -3 m interval as well, resulting in 96 ± 55 Gt in the deltaic alluvium. The Yedoma domain carbon inventories are taken from Strauss et al. (2013), Walter Anthony et al. (2014) and Fritz et al. (2015). Dotted circles represent the lower range of the estimates. There are overlaps of the pools, as the deep carbon is also calculated starting from the permafrost table and the majority of the surface pools are part of the permafrost terrain.

carbon is sequestered than released (Walter Anthony et al., 2014).

Although the first estimate of the Yedoma deposit carbon stock by Zimov et al. (2006) is now reduced by nearly a factor of two (Fig. 5), the

total Yedoma domain is still estimated to contain between 327 Gt (213 Gt (Strauss et al., 2013) plus 114 Gt taberal (Walter Anthony et al., 2014)) and 466 Gt (mean-based calculation (353 Gt (Strauss et al., 2013)) plus 114 Gt taberal) organic carbon (Fig. 7).

Given that the non-parametric (bootstrapping) calculation approach is robust with respect to skewed data and should give the same numbers if the data followed a normal distribution, we recommend using the non-parametric method. Mean calculations require a normal distribution, which is not the case especially for TOC data. Regardless of this, these numbers, derived from independent approaches and datasets, confirm that several hundred billion tons of organic carbon are stored at shallow to moderate depths in this permafrost region. Synthesizing the existing data illustrated in Fig. 5, a simple combination of the pools gives an organic carbon stocks in Yedoma deposits of 115 Gt (mean of from 71 (83 ± 12) to 150 (129 ± 30 Gt)) and 169 Gt (mean of from 100 (130 ± 30) to 237 (213 ± 24 Gt)) (Fig. 6). As a synthesis value by adding these two means of calculated ranges and including the single estimation of carbon in taberal deposits, we offer a Yedoma domain carbon inventory of 398 Gt. Even according to conservative, lower-end estimates (Strauss et al., 2013), the Yedoma and thermokarst deposits hold > 25% (213 Gt) of the frozen carbon of the circumpolar permafrost region (totally 822 Gt, Fig. 6), while covering only 7% of the soil area in this region ($17,800,000 \text{ km}^2$ (Hugelius et al., 2014)). By applying a bootstrapping approach and using the postulated late Pleistocene maximum paleo-Yedoma coverage (3.3 mio km^2 , including now flooded Arctic Ocean shelves), we estimate a last-glacial Yedoma organic carbon inventory as big as 657 ± 97 Gt.

Whether this large amount of frozen carbon may induce a strong permafrost carbon feedback to climate warming depends on its vulnerability to thaw and decomposition. The frozen deposits of the Yedoma domain alone store probably at least as much carbon as the tropical forest biomass (Lal, 2004). Nevertheless, the Yedoma domain includes additional organic carbon pools. First, there is carbon stored in the active layer. The active-layer depth in the Siberian part of the Yedoma domain is estimated to be < 0 to ~ 2 m thick (Beer et al., 2013). Assuming a mean active-layer depth of 1 m across the region, the Yedoma domain active layer includes ~ 30 Gt organic carbon (calculation based on 472 Gt for the circum-Arctic permafrost region ($18,700,000 \text{ km}^2$) (Hugelius et al., 2013)). However, large uncertainties in carbon data and the active-layer thickness remain. Active layer thickness is spatially and temporally very heterogeneous due to relief position, vegetation and soil characteristics as well as latitude and climate. Thus, the confidence in this estimate is low.

Deeper stratigraphic units consisting of frozen sediments found below Yedoma deposits (Fig. S2) also contain organic carbon (Schirrmeister et al., 2011a). While the TOC content in sandy deposits below the Yedoma is relatively low, TOC contents in Eemian thermokarst deposits are similar to Holocene thermokarst deposits, and late Saalian ice-rich deposits have TOC values similar to late Pleistocene Yedoma deposits (Schirrmeister et al., 2011a). But, due to unknown spatial coverage and thickness of these frozen deeper strata underlying Yedoma deposits, it is so far not known how much carbon may be stored below Yedoma deposits. A major question for future work could be how vulnerable this even deeper carbon is to thaw and erosion by thermokarst and thermoerosion processes.

Carbon stored in the ground ice of the Yedoma domain is another component of the inventory. Segregated ice in Yedoma from Muostakh Island (Siberia) contains 0.35 kg/m^3 dissolved organic carbon (DOC) (Fritz et al., 2015). Extrapolated from this single dataset and an estimate of $\sim 40 \text{ vol\%}$ segregated ice volume (excluding ice wedges), segregated ice in Yedoma and thermokarst deposits together may contain ~ 1 Gt DOC. Ice wedges in these deposits include DOC as well. Assuming a wedge ice volume of 48 vol% for Yedoma and 7 vol% for thermokarst deposits (Strauss et al., 2013), Yedoma ice wedges contain 0.0053 kg/m^3 and thermokarst deposit wedges 0.00051 kg/m^3 DOC (Fritz et al., 2015). Ice wedge DOC data from Alaska (Douglas et al.,

2011) and the Kolyma region in Siberia (Vonk et al., 2013b) indicate concentrations of 18.4 to 68.5 mg/l and 8.8 to 15.0 mg/l, respectively, which is comparable to a recent study (Fritz et al., 2015) (2.4 to 28.6 mg/l). Combined with deposit thickness and volumes (Strauss et al., 2013), this corresponds to approximately 0.05 Gt DOC (Fig. 7) stored in ground ice of the Yedoma domain (Fritz et al., 2015). Segregated ice and wedge ice do not contain much carbon compared to the sediment carbon pools described above.

However, high bio-decomposability of dissolved OM (Cory et al., 2014; Vonk et al., 2013a) from this pool makes this smaller pool relevant in scenarios of permafrost degradation. It is supposed that Yedoma ice-wedge melt, including its decomposable low-molecular weight compounds, has a priming effect on the decomposition of Yedoma carbon (Vonk et al., 2013b). Nevertheless, it is expected that by 2100, 5 to 10 Tg of DOC will be released from Yedoma deposits every year (Drake et al., 2015). This equals 19–26% of the annual DOC loads exported by Arctic rivers. As these numbers are based on experimental data (Drake et al., 2015) a rapid mineralization in soils and/or headwater streams was assumed. Overall, the confidence in estimates of ground ice DOC pools in the Yedoma domain is low due to very limited data. Permafrost ground ice may also contain enclosed gas bubbles, some of which contain CO₂ and CH₄. We know only one preliminary local study on this gaseous carbon amount (Brouchkov and Fukuda, 2002), which could be released during thaw directly.

5.2. Lability of organic matter: what is the vulnerability of the Yedoma domain's organic matter to future decomposition?

Because there is concern that thawing permafrost will mobilize and release old organic carbon to the atmosphere (Kuhry et al., 2013; Schuur et al., 2009), it is of high interest to assess the quality of the Yedoma domain organic carbon. It has been assumed that OM decomposability differs significantly between the Yedoma and thermokarst deposit carbon pools (Walter Anthony et al., 2014). This assumption was based on differences in permafrost OM origins for the Yedoma carbon pool and the thermokarst carbon. The Yedoma carbon was largely accumulated under aerobic conditions and likely, froze into permafrost within decades to centuries after burial. It then remained frozen for thousands of years. In contrast, Holocene thermokarst deposit carbon accumulated predominately under wetland conditions including anaerobic polygonal centres and aerobic polygon rims, or lacustrine anaerobic conditions. The lacustrine carbon remained unfrozen for centuries to millennia prior to freezing after lake drainage. A second component of the Holocene carbon pool has formed after lake drainage as an organic deposit (peat) or reworked mineral deposits under varying regimes, including both aerobic and anaerobic settings, after lake drainage.

We suggest that Yedoma deposit OM is vulnerable to microbial decomposition because it has not undergone Holocene decomposition. Due to cold and dry conditions, we assume a very low Pleistocene decomposition. However, a difference in quality and decomposability of OM from Pleistocene Yedoma and Holocene thermokarst deposits was not found (Knoblauch et al., 2013; Strauss et al., 2015). This indicates that OM vulnerability is heterogeneous and depends on ecosystem properties with different decomposition trajectories and the previous incorporation-decomposition history (Schmidt et al., 2011). Similar values with increasing age reveal that permafrost acts like a 'giant freezer', preserving the properties and composition of ancient OM. A net carbon accumulation in thermokarst basins was found since the mid Holocene (~6000 yrs BP) (Walter Anthony et al., 2014). This is supported by comparing the carbon contents of Yedoma and thermokarst deposits in an independent dataset (Strauss et al., 2013). Since OM in both Yedoma and thermokarst deposits appears to be partly in a low-decomposition state (Strauss et al., 2015), a significant vulnerability to microbial decomposition after thawing can be expected.

In this region, future deep permafrost degradation is likely as the

Yedoma domain includes large amounts of ground ice. Ongoing climate warming in the Arctic will lead to an increase in the occurrence and magnitude of disturbance processes. In particular, wildfires, thermokarst, and thermoerosional gully development will result in enhanced permafrost thaw, followed by decomposition of permafrost OM (Grosse et al., 2011b). Since microbial processes govern OM decomposition, an increase in ground temperatures will lead to higher rates of OM decomposition (Hicks Pries et al., 2013; Natali et al., 2014; Schädel et al., 2016; Schuur et al., 2009). As a result of permafrost degradation, the sequestered OM will become available to microbial decomposition and will lead to increased soil respiration, thus favouring a change from a carbon sink to a source. While the physical degradation mechanisms are well understood, the rates of OM decomposition following remobilization of previously frozen OM, especially in the Yedoma domain, are debated and subject to current research.

Based on OM concentrations in thawed samples from thermally-eroded bluffs and neglecting differences in carbon concentrations in the originally frozen material and the possibility of mixing of thawed material from different stratigraphic units (Fig. S2), it is estimated that ~60% of the Yedoma deposit organic carbon is released as CO₂ in one thawing season prior to reaching a waterbody downslope (Vonk et al., 2012). In contrast, incubation measurements indicate much lower decomposition rates of Yedoma OM. Measurements of aerobic decomposition of Yedoma OM resulted in a release of 1 to 2% of initial organic carbon as CO₂ over a period of 3 to 4 months, which represents one thawing period (Dutta et al., 2006; Knoblauch et al., 2013). At higher incubation temperatures (15 °C instead of 4–5 °C) and longer incubation periods (500 days) 11–14% of initial organic carbon from Yedoma samples was released as CO₂, which was substantially higher than CO₂ production from samples of Holocene permafrost affected mineral soils (Lee et al., 2012) subjected to the same conditions. However, for long term estimates of Yedoma OM decomposition it is necessary to consider decreasing respiration rates after the labile and readily decomposable fraction of the total organic carbon pool is respired. A two pool OM decomposition model was fitted to the cumulative CO₂ release of thawed permafrost samples from Pleistocene Yedoma and Holocene thermokarst deposits incubated at 4 °C for three years (Knoblauch et al., 2013). The model results indicated that the labile pool accounted for only about 2% of initial organic carbon when decomposition took place under aerobic conditions and only 0.6% if anaerobic conditions prevailed. The predicted release of CO₂ from the thawed permafrost samples over a period of 100 years, assuming microbial OM decomposition for four months per year, i.e. during the thaw season, was about 15% of initial organic carbon in the thawed permafrost assuming aerobic decomposition but only 2% if anoxic conditions slow down OM decomposition.

In a similar approach a three-pool (fast, slow, and passive) decomposition model was used to estimate pool sizes and turnover rates using incubation data from 23 circum-Arctic sites (Schädel et al., 2014). The fast-cycling carbon (turnover time < 1 yr at 5 °C) was found to be < 5% of initial organic carbon in the studied permafrost which is in accordance with Knoblauch et al. (2013). Up to 20% and 90% of the OM could potentially be decomposed to CO₂ within 50 incubation years at a constant temperature of 5 °C, with the highest loss in organic soils and the lowest in deep mineral soils. These values are measured with incubation under lab conditions, showing the lab potential rather than an extrapolation to real-world conditions (Schädel et al., 2014). Anyway, for Yedoma deposits, the projected carbon loss over the 50 incubation year period was 9.6% and most of the organic carbon was attributed to the passive carbon pool. Thus, based on ~10 Gt organic carbon as a basis of calculation for the first 3 m of Yedoma deposits (Hugelius et al., 2014; Strauss et al., 2013), this would mean 1 Gt organic carbon could be emitted when exposed to 5 °C for 50 years. When accounting for thermokarst deposits (~23 Gt in the first 3 m, including organic soils with higher decomposition rates), this type of deposits is projected to emit between 5 and 20 Gt carbon as CO₂ (assuming the

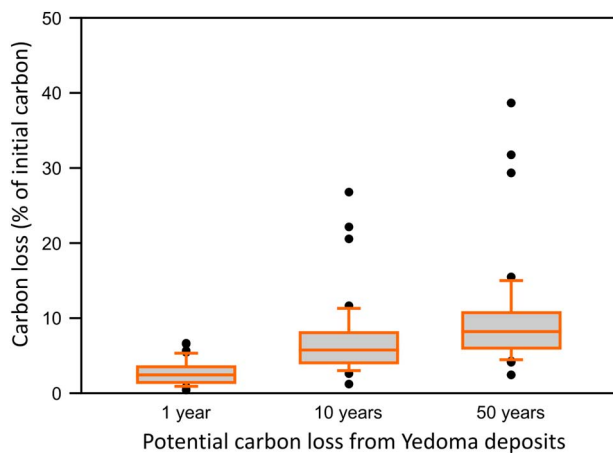


Fig. 8. Potential Yedoma carbon loss for 1, 10 and 50 incubation years at 5 °C for all long-term incubation data used in Schädel et al. (2014). For this figure 47 samples are included: 18 from Dutta et al. (2006), 25 from Knoblauch et al. (2013), and 4 from Lee et al. (2012).

published 20 to 90% decomposition rates (Schädel et al., 2014, respectively) when exposed to 5 °C for 50 years (Fig. 8). These estimations do not include thermoerosional processes, which make deeper carbon available.

A highly labile OM fraction is in DOC (Vonk et al., 2013a). Different studies reported that ancient DOC draining from deeper layers of permafrost deposit was more susceptible to decomposition by aquatic bacteria compared to modern DOC draining the shallow active layer (Mann et al., 2015; Ward and Cory, 2015). Another study (Spencer et al., 2015) found that overland flows draining Yedoma areas include a substantial amount of bio-decomposable DOC. As mentioned above, wedge-ice melt water can catalyze DOC decomposition in water bodies (Vonk et al., 2013b). Hence, the presence of substantial amounts of wedge ice in Yedoma deposits increases the vulnerability of these deposits not only to thermokarst, but also to the release of highly decomposable DOC. After entering the aquatic systems, the DOC from ancient Yedoma was found to be exceptionally bio-labile (Mann et al., 2014; Vonk et al., 2013a). Particulate organic carbon resulting from erosion may be protected from extensive decomposition by organomineral interactions, which stabilize the OM (Höfle et al., 2013) and, in aquatic environments, promote rapid settling and sedimentation (Vonk et al., 2010).

Model and data-based analyses of past warming events indicate that large amounts of OM were degraded in the past and eventually released to the atmosphere (Köhler et al., 2014). Mobilizing portions of the Yedoma carbon pool may partially explain this. During past warming events, in particular the MIS 3 interstadial and the early Holocene, considerable amounts of CH₄ were trapped in the Yedoma deposits (Bischoff et al., 2013). Moreover an analogue shift of microbial communities and an associated increase in CH₄ emission in future warming environments if permafrost thaw occurs under water saturated conditions is predicted (Bischoff et al., 2013). The pathways and fate of the lost ~200 Gt carbon from the late Pleistocene Yedoma domain since the last glacial is uncertain in detail, but in addition to that assumed to have been released to the atmosphere (Köhler et al., 2014) a portion was re-sequestered off-shore on the shelf areas (Vonk et al., 2012).

6. Implications for future carbon release from the Yedoma domain

The organic carbon pool in the Yedoma domain is subject to low mean annual ground temperatures under present day climate conditions and therefore a very large proportion of this pool is an inactive part of the global carbon cycle. After reactivation by thaw, the Yedoma domain has been suggested as one of the potential climate tipping

elements (Lenton, 2012).

To evaluate this, modelling studies try to answer the question: What will be the fate of this frozen deep carbon pool when Arctic temperatures increase in the future due to global climate warming and extensive permafrost degradation? In contrast to the usually short time span of incubation experiments of only a few weeks to months, and in exceptional cases several years, model-based studies aim to project organic carbon release on the timescale of decades to centuries (Burke et al., 2012; Schaefer et al., 2011; Schuur et al., 2015). One approach was to investigate the vulnerability of deep Yedoma permafrost carbon by accounting for the effect of microbial heat generation in the model and measurements (Hollesen et al., 2015). Yet large uncertainties exist with regards to the potential of microbial heat generation and it is questionable whether this effect could indeed lead to a self-sustained thawing of Yedoma carbon stocks (Koven et al., 2011). Moreover, rather small contributions to the atmospheric carbon content from degrading Yedoma deposit carbon stocks were found (Koven et al., 2011; Schaphoff et al., 2013). However, these models did not include fast thaw processes, such as thermokarst, that can reach deep carbon. In contrast, another modelling approach accounted for deep carbon pools as well as abrupt thaw by describing thermokarst activity in the model design (Schneider von Deimling et al., 2015). The simulation results show that deep carbon from the Yedoma domain may contribute about 25% to circum-Arctic methane release from newly thawed permafrost carbon within the 21st century. This model data suggests that the fast mobilization of carbon after abrupt thaw can affect high latitude methane fluxes significantly despite the Yedoma domain covering only about 7% of circum-Arctic permafrost region and despite the OM of this carbon store being buried deep in the frozen ground. It is suggested that a release from organic carbon stored in deep deposits of the Yedoma domain does crucially affect simulated circum-Arctic methane fluxes due to abrupt thaw under thermokarst lakes and fast propagation of sub-lake taliks (Schneider von Deimling et al., 2015). These taliks can unlock large amounts of perennially frozen deep organic carbon, revealing the need of accounting for Yedoma carbon stocks in next generation Earth-System-Models for a more complete representation of the permafrost-carbon feedback. Following Schneider von Deimling et al. (2015) and including permafrost beyond the Yedoma domain as well, the additional warming through the release from newly thawed permafrost carbon amounts to about 0.03–0.14 °C (68% ranges) by 2100, continuing with adding 0.16 to 0.39 °C to simulated global mean surface air temperatures by 2300. This will be on top of the human-induced warming, which is expected to be little < 2 °C at 2100 assuming the lowest warming pathway RCP2.6 (IPCC, 2013). Providing further quantitative estimates of the potential contribution of Yedoma domain carbon to atmospheric greenhouse gases under different warming scenarios, including deep permafrost degradation processes, is lacking right now and would be an important work for the future.

7. Summary

Permafrost is a distinct feature of the Arctic. Pleistocene ice-rich permafrost with huge ice-wedges, termed Yedoma permafrost, is widespread in Siberia and Alaska and may be especially prone to thawing. Yedoma formation during the late Pleistocene was likely dominated by water-related as well as aeolian processes under very cold glacial climate and periglacial landscape conditions. Currently freeze-locked organic matter can be remobilized and contribute to a carbon-climate feedback. Estimates of the organic carbon stocks in Yedoma deposits are between 83 ± 12 and 129 ± 30 Gt. During the last glacial period Yedoma deposits potentially stored about 657 ± 97 Gt. When including deposits in degradation features, such as thermokarst lakes and basins, we found ~398 gigatons of thaw-susceptible carbon in the Yedoma domain, which is > 25% of the frozen carbon of the permafrost area, while covering only 7% of this region. Greenhouse emissions from enlarging lakes and new wetlands, caused by e.g. by

thermokarst and thermo-erosional processes, are the key process to unlock this dormant Yedoma carbon pool. Over millennia this carbon could potentially be released, but that rates of release in the coming century are likely to be orders of magnitudes lower than current human-caused emissions, but persistent and increasing in the future.

Acknowledgments

This synthesis was conducted within the Action Group “The Yedoma Region: A Synthesis of Circum-Arctic Distribution and Thickness” (funded by the International Permafrost Association) and the Permafrost Carbon Network (working group Deep Carbon Stocks). We acknowledge the support by the European Research Council (Starting Grant #338335), the German Federal Ministry of Education and Research (Grant 01DM12011 and “CarboPerm” (03G0836A)), the Initiative and Networking Fund of the Helmholtz Association (#ERC-0013), the German Research Foundation (DFG UL426/1-1) and the German Federal Environment Agency (UBA, project UFOPLAN FKZ 3712 41 106). E. Mauclet and S. Opfergelt are acknowledged for contributing data and interpretation for a Yedoma mineralogy case study (Fig. S4).

Appendix A. Supplementary data

Supplementary data to this article can be found online at <http://dx.doi.org/10.1016/j.earscirev.2017.07.007>.

References

- Andreev, A.A., Grosse, G., Schirmermeister, L., Kuznetsova, T.V., Kuzmina, S.A., Bobrov, A.A., Tarasov, P.E., Novenko, E.Y., Meyer, H., Derevyagin, A.Y., Kienast, F., Bryantseva, A., Kunitsky, V.V., 2009. Weichselian and Holocene palaeoenvironmental history of the Bol'shoy Lyakhovskiy Island, New Siberian Archipelago, Arctic Siberia. *Boreas* 38 (1), 72–110.
- Batjes, N.H., 2016. Harmonized soil property values for broad-scale modelling (WISE30sec) with estimates of global soil carbon stocks. *Geoderma* 269, 61–68. <http://dx.doi.org/10.1016/j.geoderma.2016.01.034>.
- Beer, C., Fedorov, A.N., Torgovkin, Y., 2013. Permafrost temperature and active-layer thickness of Yakutia with 0.5-degree spatial resolution for model evaluation. *Earth Syst. Sci. Data* 5 (2), 305–310. <http://dx.doi.org/10.5194/essd-5-305-2013>.
- Bischoff, J., Mangelsdorf, K., Gattinger, A., Schlöter, M., Kurchatova, A.N., Herzschuh, U., Wagner, D., 2013. Response of methanogenic archaea to Late Pleistocene and Holocene climate changes in the Siberian Arctic. *Glob. Biogeochem. Cycles* 27 (2), 305–317. <http://dx.doi.org/10.1029/2011gb004238>.
- Brosius, L.S., Walter Anthony, K.M., Grosse, G., Chanton, J.P., Farquharson, L.M., Overduin, P.P., Meyer, H., 2012. Using the deuterium isotope composition of permafrost meltwater to constrain thermokarst lake contributions to atmospheric CH₄ during the last deglaciation. *J. Geophys. Res. Biogeosci.* 117 (G1), G01022. <http://dx.doi.org/10.1029/2011jg001810>.
- Brouchkov, A., Fukuda, M., 2002. Preliminary measurements on methane content in permafrost, Central Yakutia, and some experimental data. *Permafrost. Periglac. Process.* 13 (3), 187–197. <http://dx.doi.org/10.1002/ppp.422>.
- Brown, A., 2013. Permafrost carbon storage: Pandora's freezer? *Nat. Clim. Chang.* 3 (5), 442. <http://dx.doi.org/10.1038/nclimate1896>.
- Brown, J., Ferrians, O.J., Heginbottom, J.A., Melnikov, E.S., 1998. *Circum-arctic Map of Permafrost and Ground-ice Conditions*. National Snow and Ice Data Center/World Data Center for Glaciology, Boulder, Colorado.
- Burke, E.J., Hartley, I.P., Jones, C.D., 2012. Uncertainties in the global temperature change caused by carbon release from permafrost thawing. *Cryosphere* 6 (5), 1063–1076. <http://dx.doi.org/10.5194/tc-6-1063-2012>.
- Ciais, P., Sabine, C., Bala, G., Bopp, L., Brovkin, V., Canadell, J., Chhabra, A., DeFries, R., Galloway, J., Heimann, M., Jones, C., Le Quéré, C., Myneni, R.B., Piao, S., Thornton, P., 2013. Carbon and other biogeochemical cycles. In: Stocker, T.F., Qin, D., Plattner, G.-K., Tignor, M., Allen, S.K., Boschung, J., Nauels, A., Xia, Y., Bex, V., Midgley, P.M. (Eds.), *Climate Change 2013: The Physical Science Basis*. Contribution of Working Group I to the Fifth Assessment Report of the Intergovernmental Panel on Climate Change. Cambridge University Press, Cambridge, United Kingdom and New York, USA.
- Cory, R.M., Ward, C.P., Crump, B.C., Kling, G.W., 2014. Sunlight controls water column processing of carbon in Arctic fresh waters. *Science* 345 (6199), 925–928. <http://dx.doi.org/10.1126/science.1253119>.
- Douglas, T.A., Fortier, D., Shur, Y.L., Kanevskiy, M.Z., Guo, L., Cai, Y., Bray, M.T., 2011. Biogeochemical and geocryological characteristics of wedge and thermokarst-cave ice in the CREEL permafrost tunnel, Alaska. *Permafrost. Periglac. Process.* 22 (2), 120–128. <http://dx.doi.org/10.1002/ppp.709>.
- Drake, T.W., Wickland, K.P., Spencer, R.G.M., McKnight, D.M., Striegl, R.G., 2015. Ancient low-molecular-weight organic acids in permafrost fuel rapid carbon dioxide production upon thaw. *Proc. Natl. Acad. Sci.* 112 (45), 13946–13951. <http://dx.doi.org/10.1073/pnas.1511705112>.
- Dutta, K., Schuur, E.A.G., Neff, J.C., Zimov, S.A., 2006. Potential carbon release from permafrost soils of Northeastern Siberia. *Glob. Chang. Biol.* 12 (12), 2336–2351. <http://dx.doi.org/10.1111/j.1365-2486.2006.01259.x>.
- Euskirchen, E.S., Goodstein, E.S., Huntington, H.P., 2013. An estimated cost of lost climate regulation services caused by thawing of the Arctic cryosphere. *Ecol. Appl.* 23 (8), 1869–1880. <http://dx.doi.org/10.1890/11-0858.1>.
- Fritz, M., Opel, T., Tanski, G., Herzschuh, U., Meyer, H., Eulenburg, A., Lantuit, H., 2015. Dissolved organic carbon (DOC) in Arctic ground ice. *Cryosphere* 9, 737–752. <http://dx.doi.org/10.5194/tc-9-737-2015>.
- Froese, D.G., Zazula, G.D., Westgate, J.A., Preece, S.J., Sanborn, P.T., Reyes, A.V., Pearce, N.J., 2009. The Klondike goldfields and Pleistocene environments of Beringia. *GSA Today* 19 (8), 4–10. <http://dx.doi.org/10.1130/GSATG54A.1>.
- Grosse, G., Romanovsky, V., Jorgenson, T., Anthony, K.W., Brown, J., Overduin, P.P., 2011a. Vulnerability and feedbacks of permafrost to climate change. *EOS Trans. Am. Geophys. Union* 92 (9), 73–74. <http://dx.doi.org/10.1029/2011eo090001>.
- Grosse, G., Harden, J., Turetsky, M.R., McGuire, A.D., Camill, P., Tarnocai, C., Froking, S., Schuur, E.A.G., Jorgenson, T., Marchenko, S., Romanovsky, V., Wickland, K.P., French, N., Waldrop, M.P., Bourgeau-Chavez, L., Striegl, R.G., 2011b. Vulnerability of high-latitude soil organic carbon in North America to disturbance. *J. Geophys. Res. Biogeosci.* 116, G00K06. <http://dx.doi.org/10.1029/2010JG001507>.
- Grosse, G., Robinson, J.E., Bryant, R., Taylor, M.D., Harper, W., DeMasi, A., Kyker-Snowman, E., Veremeeva, A., Schirmermeister, L., Harden, J., 2013. Distribution of late Pleistocene ice-rich syngenetic permafrost of the Yedoma Suite in east and central Siberia, Russia. In: *US Geological Survey Open File Report, 1078*. U.S. Geological Survey, Reston, Virginia (37 pp).
- Günther, F., Overduin, P.P., Sandakov, A.V., Grosse, G., Grigoriev, M.N., 2013. Short- and long-term thermo-erosion of ice-rich permafrost coasts in the Laptev Sea region. *Biogeosciences* 10 (6), 4297–4318. <http://dx.doi.org/10.5194/bg-10-4297-2013>.
- Günther, F., Overduin, P.P., Yakshina, I.A., Opel, T., Baranskaya, A.V., Grigoriev, M.N., 2015. Observing Muostakh disappear: permafrost thaw subsidence and erosion of a ground-ice-rich island in response to Arctic summer warming and sea ice reduction. *Cryosphere* 9 (1), 151–178. <http://dx.doi.org/10.5194/tc-9-151-2015>.
- Hayes, D.J., McGuire, A.D., Kicklighter, D.W., Gurney, K.R., Burnside, T.J., Melillo, J.M., 2011. Is the northern high-latitude land-based CO₂ sink weakening? *Glob. Biogeochem. Cycles* 25 (3), GB3018. <http://dx.doi.org/10.1029/2010gb003813>.
- Hicks Pries, C.E., Schuur, E.A.G., Crummer, K.G., 2013. Thawing permafrost increases old soil and autotrophic respiration in tundra: partitioning ecosystem respiration using $\delta^{13}\text{C}$ and $\Delta^{14}\text{C}$. *Glob. Chang. Biol.* 19 (2), 649–661. <http://dx.doi.org/10.1111/gcb.12058>.
- Hinkel, K.M., Nelson, F.E., 2003. Spatial and temporal patterns of active layer thickness at Circumpolar Active Layer Monitoring (CALM) sites in northern Alaska, 1995–2000. *J. Geophys. Res. Atmos.* 108 (D2), 8168. <http://dx.doi.org/10.1029/2001jd000927>.
- Höfle, S., Rethemeyer, J., Mueller, C.W., John, S., 2013. Organic matter composition and stabilization in a polygonal tundra soil of the Lena Delta. *Biogeosciences* 10 (5), 3145–3158. <http://dx.doi.org/10.5194/bg-10-3145-2013>.
- Hollesen, J., Matthiesen, H., Møller, A.B., Elberling, B., 2015. Permafrost thawing in organic Arctic soils accelerated by ground heat production. *Nat. Clim. Chang.* 5 (6), 574–578. <http://dx.doi.org/10.1038/nclimate2590>.
- Hubberten, H.W., Andreev, A., Astakhov, V.I., Demidov, I., Dowdeswell, J.A., Henriksen, M., Hjort, C., Houmark-Nielsen, M., Jakobsson, M., Kuzmina, S., Larsen, E., Pekka Lunkka, J., Lysa, A., Mangerud, J., Möller, P., Saarnisto, M., Schirmermeister, L., Sher, A.V., Siegert, C., Siegert, M.J., Svendsen, J.I., 2004. The periglacial climate and environment in northern Eurasia during the Last Glaciation. *Quat. Sci. Rev.* 23 (11–13), 1333–1357. <http://dx.doi.org/10.1016/j.quascirev.2003.12.012>.
- Hugelius, G., Bockheim, J.G., Camill, P., Elberling, B., Grosse, G., Harden, J.W., Johnson, K., Jorgenson, T., Koven, C.D., Kuhry, P., Michaelson, G., Mishra, U., Palmtag, J., Ping, C.-L., O'Donnell, J., Schirmermeister, L., Schuur, E.A.G., Sheng, Y., Smith, L.C., Strauss, J., Yu, Z., 2013. A new data set for estimating organic carbon storage to 3 m depth in soils of the northern circumpolar permafrost region. *Earth Syst. Sci. Data* 5, 393–402. <http://dx.doi.org/10.5194/essd-5-393-2013>.
- Hugelius, G., Strauss, J., Zubrzycki, S., Harden, J., Schuur, E.A.G., Ping, C.-L., Schirmermeister, L., Grosse, G., Michaelson, G., Koven, C., O'Donnell, J., Elberling, B., Mishra, U., Camill, P., Yu, Z., Palmtag, J., Kuhry, P., 2014. Estimated stocks of circumpolar permafrost carbon with quantified uncertainty ranges and identified data gaps. *Biogeosciences* 11, 6573–6593. <http://dx.doi.org/10.5194/bg-11-6573-2014>.
- IPCC, 2013. In: Stocker, T.F., Qin, D., Plattner, G.-K., Tignor, M., Allen, S.K., Boschung, J., Nauels, A., Xia, Y., Bex, V., Midgley, P.M. (Eds.), *Climate Change 2013: The Physical Science Basis*. Contribution of Working Group I to the Fifth Assessment Report of the Intergovernmental Panel on Climate Change. Cambridge University Press, Cambridge, United Kingdom and New York, USA, pp. 1535.
- Jobbágy, E.G., Jackson, R.B., 2000. The vertical distribution of soil organic carbon and its relation to climate and vegetation. *Ecol. Appl.* 10 (2), 423–436. [http://dx.doi.org/10.1890/1051-0761\(2000\)010\[0423:TVDOSO\]2.0.CO;2](http://dx.doi.org/10.1890/1051-0761(2000)010[0423:TVDOSO]2.0.CO;2).
- Jones, B.M., Grosse, G., Arp, C.D., Jones, M.C., Walter Anthony, K.M., Romanovsky, V.E., 2011. Modern thermokarst lake dynamics in the continuous permafrost zone, northern Seward Peninsula, Alaska. *J. Geophys. Res. Biogeosci.* 116, G00M03. <http://dx.doi.org/10.1029/2011JG001666>.
- Kanevskiy, M., Shur, Y., Fortier, D., Jorgenson, M.T., Stephani, E., 2011. Cryostratigraphy of late Pleistocene syngenetic permafrost (yedoma) in northern Alaska, Itkillik River exposure. *Quat. Res.* 75 (3), 584–596. <http://dx.doi.org/10.1016/j.yqres.2010.12.003>.
- Kanevskiy, M., Jorgenson, T., Shur, Y., O'Donnell, J.A., Harden, J.W., Zhuang, Q., Fortier, D., 2014. Cryostratigraphy and permafrost evolution in the lacustrine lowlands of west-central Alaska. *Permafrost. Periglac. Process.* 25 (1), 14–34. <http://dx.doi.org/10.1002/ppp.709>.

- 1002/ppp.1800.
- Kanevskiy, M., Shur, Y.L., Strauss, J., Jorgenson, M.T., Fortier, D., Stephani, E., Vasiliev, A., 2016. Patterns and rates of riverbank erosion in the area of ice-rich permafrost (yedoma) in northern Alaska. *Geomorphology* 253, 370–384. <http://dx.doi.org/10.1016/j.geomorph.2015.10.023>.
- Kaplina, T.N., 1981. Istoriya merzlykh tolschch severnoy Yakutii v pozdnyom kaynozoye (the history of permafrost in North Yakutia during the late Cenozoic). In: Dubikov, G.I., Baulin, V.V. (Eds.), *Istoriya razvitiya mnogolyetnemerzlykh porod Yevrazii (The History of the Development of Perennially Frozen Deposits in Eurasia)*. Nauka, Moscow, pp. 153–181.
- Kaplina, T.N., Giterman, R.E., Lakhtina, O.V., Abrashov, B.A., Kiselyov, S.V., Sher, A.V., 1978. Duvanny Yar - a key section of Upper Pleistocene deposits of the Kolyma lowland. *Bulletin of Quat. Res. Comm.* 48, 49–65.
- Knoblauch, C., Beer, C., Sosnin, A., Wagner, D., Pfeiffer, E.-M., 2013. Predicting long-term carbon mineralization and trace gas production from thawing permafrost of Northeast Siberia. *Glob. Chang. Biol.* 19 (4), 1160–1172. <http://dx.doi.org/10.1111/gcb.12116>.
- Köchy, M., Hiederer, R., Freibauer, A., 2015. Global distribution of soil organic carbon – part 1: masses and frequency distributions of SOC stocks for the tropics, permafrost regions, wetlands, and the world. *Soil* 1 (1), 351–365. <http://dx.doi.org/10.5194/soil-1-351-2015>.
- Köhler, P., Knorr, G., Bard, E., 2014. Permafrost thawing as a possible source of abrupt carbon release at the onset of the Bølling/Allerød. *Nat. Commun.* 5. <http://dx.doi.org/10.1038/ncomms6520>.
- Koven, C.D., Ringeval, B., Friedlingstein, P., Ciais, P., Cadule, P., Khvorostyanov, D., Krinner, G., Tarnocai, C., 2011. Permafrost carbon-climate feedbacks accelerate global warming. *Proc. Natl. Acad. Sci.* 108 (36), 14769–14774. <http://dx.doi.org/10.1073/pnas.1103910108>.
- Koven, C.D., Schuur, E.A.G., Schädel, C., Bohn, T.J., Burke, E.J., Chen, G., Chen, X., Ciais, P., Grosse, G., Harden, J.W., Hayes, D.J., Hugelius, G., Jafarov, E.E., Krinner, G., Kuhry, P., Lawrence, D.M., MacDougall, A.H., Marchenko, S.S., McGuire, A.D., Natali, S.M., Nicolsky, D.J., Olefeldt, D., Peng, S., Romanovsky, V.E., Schaefer, K.M., Strauss, J., Treat, C.C., 2015. A simplified, data-constrained approach to estimate the permafrost carbon-climate feedback. *Philos. Trans. R. Soc. A Math. Phys. Eng. Sci.* 373, 20140423. <http://dx.doi.org/10.1098/rsta.2014.0423>.
- Kuhry, P., Grosse, G., Harden, J.W., Hugelius, G., Koven, C.D., Ping, C.L., Schirrmeister, L., Tarnocai, C., 2013. Characterisation of the permafrost carbon pool. *Permafrost. Periglac. Process.* 24 (2), 146–155. <http://dx.doi.org/10.1002/ppp.1782>.
- Kurylyk, B.L., Hayashi, M., Quinton, W.L., McKenzie, J.M., Voss, C.I., 2016. Influence of vertical and lateral heat transfer on permafrost thaw, peatland landscape transition, and groundwater flow. *Water Resour. Res.* 52 (2), 1286–1305. <http://dx.doi.org/10.1002/2015WR018057>.
- Kutzbach, L., Wille, C., Pfeiffer, E.M., 2007. The exchange of carbon dioxide between wet Arctic tundra and the atmosphere at the Lena River Delta, Northern Siberia. *Biogeosciences* 4 (5), 869–890. <http://dx.doi.org/10.5194/bg-4-869-2007>.
- Kuzmina, S.A., Sher, A.V., Edwards, M.E., Haile, J., Yan, E.V., Kotov, A.V., Willerslev, E., 2011. The late Pleistocene environment of the Eastern West Beringia based on the principal section at the Main River, Chukotka. *Quat. Sci. Rev.* 30 (17–18), 2091–2106. <http://dx.doi.org/10.1016/j.quascirev.2010.03.019>.
- Lal, R., 2004. Soil carbon sequestration in natural and managed tropical forest ecosystems. *J. Sustain. For.* 21 (1), 1–30. http://dx.doi.org/10.1300/J091v21n01_01.
- Lee, H., Schuur, E.A.G., Inglett, K.S., Lavoie, M., Chanton, J.P., 2012. The rate of permafrost carbon release under aerobic and anaerobic conditions and its potential effects on climate. *Glob. Chang. Biol.* 18 (2), 515–527. <http://dx.doi.org/10.1111/j.1365-2486.2011.02519.x>.
- Lenton, T.M., 2012. Arctic climate tipping points. *Ambio* 41 (1), 10–22. <http://dx.doi.org/10.1007/s13280-011-0221-x>.
- Lindgren, A., Hugelius, G., Kuhry, P., Christensen, T.R., Vandenbergh, J., 2015. GIS-based maps and area estimates of northern hemisphere permafrost extent during the last glacial maximum. *Permafrost. Periglac. Process.* 6–16. <http://dx.doi.org/10.1002/ppp.1851>.
- Mackelprang, R., Waldrop, M.P., DeAngelis, K.M., David, M.M., Chavarria, K.L., Blazewicz, S.J., Rubin, E.M., Jansson, J.K., 2011. Metagenomic analysis of a permafrost microbial community reveals a rapid response to thaw. *Nature* 480 (7377), 368–371. <http://dx.doi.org/10.1038/nature10576>.
- Mann, P.J., Sobczak, W.V., LaRue, M.M., Bulygina, E., Davydova, A., Vonk, J.E., Schade, J., Davydov, S., Zimov, N., Holmes, R.M., Spencer, R.G.M., 2014. Evidence for key enzymatic controls on metabolism of Arctic river organic matter. *Glob. Chang. Biol.* 20 (4), 1089–1100. <http://dx.doi.org/10.1111/gcb.12416>.
- Mann, P.J., Eglinton, T.L., McIntyre, C.P., Zimov, N., Davydova, A., Vonk, J.E., Holmes, R.M., Spencer, R.G.M., 2015. Utilization of ancient permafrost carbon in headwaters of Arctic fluvial networks. *Nat. Commun.* 6. <http://dx.doi.org/10.1038/ncomms8856>.
- Mascarelli, A., 2009. A sleeping giant? *Nat. Rep. Clim. Change* 3 (4), 46–49. <http://dx.doi.org/10.1038/climate.2009.24>.
- McGuire, A.D., Macdonald, R.W., Schuur, E.A.G., Harden, J.W., Kuhry, P., Hayes, D.J., Christensen, T.R., Heimann, M., 2010. The carbon budget of the northern cryosphere region. *Curr. Opin. Environ. Sustain.* 2 (4), 231–236. <http://dx.doi.org/10.1016/j.cosust.2010.05.003>.
- Morgenstern, A., Ulrich, M., Günther, F., Roessler, S., Fedorova, I.V., Rudaya, N.A., Wetterich, S., Boike, J., Schirrmeister, L., 2013. Evolution of thermokarst in East Siberian ice-rich permafrost: a case study. *Geomorphology* 201 (0), 363–379. <http://dx.doi.org/10.1016/j.geomorph.2013.07.011>.
- Muhs, D.R., Bettis, E., 2003. Quaternary loess-paleosol sequences as examples of climate-driven sedimentary extremes. In: Chan, M.A., Archer, A.W. (Eds.), *Extreme Depositional Environments: Mega End Members in Geologic Time*. Geological Society of America Special Paper 370. Geological Society of America, Boulder, Colorado, pp. 53–74.
- Murton, J.B., Goslar, T., Edwards, M.E., Bateman, M.D., Danilov, P.P., Savvinov, G.N., Gubin, S.V., Ghaleb, B., Haile, J., Kanevskiy, M., Lozhkin, A.V., Lupachev, A.V., Murton, D.K., Shur, Y., Tikhonov, A., Vasil'chuk, A.C., Vasil'chuk, Y.K., Wolfe, S.A., 2015. Palaeoenvironmental interpretation of Yedoma silt (Ice Complex) deposition as cold-climate loess, Duvanny Yar, Northeast Siberia. *Permafrost. Periglac. Process.* 26 (3), 208–288. <http://dx.doi.org/10.1002/ppp.1843>.
- Natali, S.M., Schuur, E.A.G., Webb, E.E., Pries, C.E.H., Crummer, K.G., 2014. Permafrost degradation stimulates carbon loss from experimentally warmed tundra. *Ecology* 95 (3), 602–608. <http://dx.doi.org/10.1890/13-0602.1>.
- Olefeldt, D., Goswami, S., Grosse, G., Hayes, D., Hugelius, G., Kuhry, P., McGuire, A.D., Romanovsky, V.E., Sannel, A.B.K., Schuur, E.A.G., Turetsky, M.R., 2016. Circumpolar distribution and carbon storage of thermokarst landscapes. *Nat. Commun.* 7, 13043. <http://dx.doi.org/10.1038/ncomms13043>.
- Overland, J., Hanna, E., Hanssen-Bauer, I., Kim, S.-J., Walsh, J.E., Wang, M., Bhatt, U.S., Thoman, R.L., 2015. Surface air temperature. In: *Arctic Report Card: Update 2015 - Tracking Recent Environmental Changes*. Arctic Research Program in the National Oceanic and Atmospheric Administration, U.S. Department of Commerce, Washington.
- Pécsi, M., 1990. Loess is not just accumulation of airborne dust. *Quat. Int.* 7 (8), 1–21.
- Péwé, T.L., 1955. Origin of the upland silt near Fairbanks, Alaska. *Geol. Soc. Am. Bull.* 66 (6), 699–724. [http://dx.doi.org/10.1130/0016-7606\(1955\)66\[699:ootusn\]2.0.co;2](http://dx.doi.org/10.1130/0016-7606(1955)66[699:ootusn]2.0.co;2).
- Péwé, T.L., 1975. Quaternary geology of Alaska. *US Geol. Surv. Prof. Pap.* 835.
- Péwé, T.L., Journaux, A., 1983. Origin and character of loesslike silt in unglaciated south-central Yakutia, Siberia, USSR. *US Geol. Surv. Prof. Pap.* 1262.
- Romanovskii, N.N., 1993. *Fundamentals of Cryogenesis of Lithosphere*. Moscow University Press, Moscow.
- Romanovsky, V.E., Drozdov, D.S., Oberman, N.G., Malkova, G.V., Kholodov, A.L., Marchenko, S.S., Moskalenko, N.G., Sergeev, D.O., Ukrainseva, N.G., Abramov, A.A., Gilchenko, D.A., Vasiliev, A.A., 2010. Thermal state of permafrost in Russia. *Permafrost. Periglac. Process.* 21 (2), 136–155. <http://dx.doi.org/10.1002/ppp.683>.
- Sanborn, P.T., Smith, C.A.S., Froese, D.G., Zazula, G.D., Westgate, J.A., 2006. Full-glacial paleosols in perennially frozen loess sequences, Klondike goldfields, Yukon Territory, Canada. *Quat. Res.* 66 (1), 147–157. <http://dx.doi.org/10.1016/j.yqres.2006.02.008>.
- Schädel, C., Schuur, E.A.G., Bracho, R., Elberling, B., Knoblauch, C., Lee, H., Luo, Y.Q., Shaver, G.R., Turetsky, M.R., 2014. Circumpolar assessment of permafrost C quality and its vulnerability over time using long-term incubation data. *Glob. Chang. Biol.* 20 (2), 641–652. <http://dx.doi.org/10.1111/gcb.12417>.
- Schädel, C., Bader, M.K.F., Schuur, E.A.G., Biasi, C., Bracho, R., Capek, P., De Baets, S., Diakova, K., Ernakovich, J., Estop-Aragones, C., Graham, D.E., Hartley, I.P., Iversen, C.M., Kane, E., Knoblauch, C., Lupasco, M., Martikainen, P.J., Natali, S.M., Norby, R.J., O'Donnell, J.A., Chowdhury, T.R., Santruckova, H., Shaver, G., Sloan, V.L., Treat, C.C., Turetsky, M.R., Waldrop, M.P., Wickland, K.P., 2016. Potential carbon emissions dominated by carbon dioxide from thawed permafrost soils. *Nat. Clim. Chang.* 6, 950–953. <http://dx.doi.org/10.1038/nclimate3054>.
- Schaefer, K., Zhang, T., Bruhwiler, L., Barrett, A.P., 2011. Amount and timing of permafrost carbon release in response to climate warming. *Tellus B* 63 (2), 165–180. <http://dx.doi.org/10.1111/j.1600-0889.2011.00527.x>.
- Schaphoff, S., Heyder, U., Ostberg, S., Gerten, D., Heinke, J., Lucht, W., 2013. Contribution of permafrost soils to the global carbon budget. *Environ. Res. Lett.* 8 (1), 014026. <http://dx.doi.org/10.1088/1748-9326/8/1/014026>.
- Schirrmeister, L., Siegert, C., Kuznetsova, T., Kuzmina, S., Andreev, A., Kienast, F., Meyer, H., Bobrov, A., 2002. Paleoenvironmental and paleoclimatic records from permafrost deposits in the Arctic region of Northern Siberia. *Quat. Int.* 89 (1), 97–118. [http://dx.doi.org/10.1016/S1040-6182\(01\)00083-0](http://dx.doi.org/10.1016/S1040-6182(01)00083-0).
- Schirrmeister, L., Kunitzky, V., Grosse, G., Wetterich, S., Meyer, H., Schwaborn, G., Babyi, O., Derevyagin, A., Siegert, C., 2011a. Sedimentary characteristics and origin of the Late Pleistocene Ice Complex on north-east Siberian Arctic coastal lowlands and islands - a review. *Quat. Int.* 241 (1–2), 3–25. <http://dx.doi.org/10.1016/j.quaint.2010.04.004>.
- Schirrmeister, L., Grosse, G., Wetterich, S., Overduin, P.P., Strauss, J., Schuur, E.A.G., Hubberten, H.-W., 2011b. Fossil organic matter characteristics in permafrost deposits of the northeast Siberian Arctic. *J. Geophys. Res. Biogeosci.* 116, G00M02. <http://dx.doi.org/10.1029/2011jg001647>.
- Schirrmeister, L., Froese, D.G., Tumskey, V., Grosse, G., Wetterich, S., 2013. Yedoma: Late Pleistocene ice-rich syngenetic permafrost of Beringia. In: Elias, S. (Ed.), *Encyclopedia of Quaternary Sciences*. Elsevier, Amsterdam, pp. 542–552.
- Schmidt, M.W.I., Torn, M.S., Abiven, S., Dittmar, T., Guggenberger, G., Janssens, I.A., Kleber, M., Kogel-Knabner, I., Lehmann, J., Manning, D.A.C., Nannipieri, P., Rasse, D.P., Weiner, S., Trumbore, S.E., 2011. Persistence of soil organic matter as an ecosystem property. *Nature* 478 (7367), 49–56.
- Schneider von Deimling, T., Grosse, G., Strauss, J., Schirrmeister, L., Morgenstern, A., Schaphoff, S., Meinshausen, M., Boike, J., 2015. Observation-based modeling of permafrost carbon fluxes with accounting for deep carbon deposits and thermokarst activity. *Biogeosciences* 12, 3469–3488. [doi:10.5194/bg-12-3469-2015](http://dx.doi.org/10.5194/bg-12-3469-2015).
- Schuur, E.A.G., Bockheim, J., Canadell, J.G., Euskirchen, E., Field, C.B., Goryachkin, S.V., Hagemann, S., Kuhry, P., Lafleur, P.M., Lee, H., 2008. Vulnerability of permafrost carbon to climate change: implications for the global carbon cycle. *Bioscience* 58 (8), 701–714. <http://dx.doi.org/10.1641/B580807>.
- Schuur, E.A.G., Vogel, J.G., Crummer, K.G., Lee, H., Sickman, J.O., Osterkamp, T.E., 2009. The effect of permafrost thaw on old carbon release and net carbon exchange from tundra. *Nature* 459 (7246), 556–559. <http://dx.doi.org/10.1038/nature08031>.
- Schuur, E.A.G., McGuire, A.D., Schädel, C., Grosse, G., Harden, J.W., Hayes, D.J., Hugelius, G., Koven, C.D., Kuhry, P., Lawrence, D.M., Natali, S.M., Olefeldt, D., Romanovsky, V.E., Schaefer, K., Turetsky, M.R., Treat, C.C., Vonk, J.E., 2015. Climate

- change and the permafrost carbon feedback. *Nature* 520 (7546), 171–179. <http://dx.doi.org/10.1038/nature14338>.
- Sher, A.V., 1971. Mammals and Stratigraphy of the Pleistocene of the Extreme Northeast of the USSR and North America. Nauka, Moscow.
- Sher, A.V., 1995. Is there any real evidence for a huge shelf ice sheet in East Siberia? *Quat. Int.* 28, 39–40.
- Sher, A.V., 1997. Yedoma as a store of paleoenvironmental records in Beringia. In: Elias, S., Brigham-Grette, J. (Eds.), *Beringia Paleoenvironmental Workshop*, Florissant, pp. 92–94.
- Spencer, R.G.M., Mann, P.J., Dittmar, T., Eglinton, T.I., McIntyre, C., Holmes, R.M., Zimov, N., Stubbins, A., 2015. Detecting the signature of permafrost thaw in Arctic rivers. *Geophys. Res. Lett.* 42 (8), 2015GL063498. <http://dx.doi.org/10.1002/2015GL063498>.
- Strauss, J., Schirrmeister, L., Wetterich, S., Borchers, A., Davydov, S.P., 2012. Grain-size properties and organic-carbon stock of Yedoma Ice Complex permafrost from the Kolyma lowland, northeastern Siberia. *Glob. Biogeochem. Cycles* 26 (3), GB3003. <http://dx.doi.org/10.1029/2011GB004104>.
- Strauss, J., Schirrmeister, L., Grosse, G., Wetterich, S., Ulrich, M., Herzschuh, U., Hubberten, H.-W., 2013. The deep permafrost carbon pool of the Yedoma region in Siberia and Alaska. *Geophys. Res. Lett.* 40, 6165–6170. <http://dx.doi.org/10.1002/2013GL058088>.
- Strauss, J., Schirrmeister, L., Mangelsdorf, K., Eichhorn, L., Wetterich, S., Herzschuh, U., 2015. Organic matter quality of deep permafrost carbon - a study from Arctic Siberia. *Biogeochemistry* 12, 2227–2245. <http://dx.doi.org/10.5194/bg-12-2227-2015>.
- Sun, D., Bloemendal, J., Rea, D.K., An, Z., Vandenberghe, J., Lu, H., Su, R., Liu, T., 2004. Bimodal grain-size distribution of Chinese loess, and its palaeoclimatic implications. *Catena* 55 (3), 325–340. [http://dx.doi.org/10.1016/S0341-8162\(03\)00109-7](http://dx.doi.org/10.1016/S0341-8162(03)00109-7).
- Tomirdiario, S.V., 1980. *Loess-ice Formations in East Siberia During the Late Pleistocene and Holocene*. Nauka Press, Moscow.
- Tomirdiario, S.V., Chernen'kiy, B.I., 1987. *Cryogenic Deposits of East Arctic and Sub Arctic*. AN SSSR Far-East-Science Centre (196 pp).
- Treat, C.C., Frolking, S., 2013. Carbon storage: a permafrost carbon bomb? *Nat. Clim. Chang.* 3 (10), 865–867. <http://dx.doi.org/10.1038/nclimate2010>.
- Turney, C.S.M., Jones, R.T., 2010. Does the Agulhas Current amplify global temperatures during super-interglacials? *J. Quat. Sci.* 25 (6), 839–843. <http://dx.doi.org/10.1002/jqs.1423>.
- Ulrich, M., Grosse, G., Strauss, J., Schirrmeister, L., 2014. Quantifying wedge-ice volumes in Yedoma and thermokarst basin deposits. *Permafr. Periglac. Process.* 25 (3), 151–161. <http://dx.doi.org/10.1002/ppp.1810>.
- van der Molen, M.K., van Huissteden, J., Parmentier, F.J.W., Petrescu, A.M.R., Dolman, A.J., Maximov, T.C., Kononov, A.V., Karsanaev, S.V., Suzdalov, D.A., 2007. The growing season greenhouse gas balance of a continental tundra site in the Indigirka lowlands, NE Siberia. *Biogeochemistry* 4 (6), 985–1003. <http://dx.doi.org/10.5194/bg-4-985-2007>.
- van Huissteden, J., Dolman, A.J., 2012. Soil carbon in the Arctic and the permafrost carbon feedback. *Curr. Opin. Environ. Sustain.* 4 (5), 545–551. <http://dx.doi.org/10.1016/j.cosust.2012.09.008>.
- Vonk, J.E., Sánchez-García, L., Semiletov, I., Dudarev, O., Eglinton, T., Andersson, A., Gustafsson, Ö., 2010. Molecular and radiocarbon constraints on sources and degradation of terrestrial organic carbon along the Kolyma paleoriver transect, East Siberian Sea. *Biogeochemistry* 7 (10), 3153–3166. <http://dx.doi.org/10.5194/bg-7-3153-2010>.
- Vonk, J.E., Sanchez-Garcia, L., van Dongen, B.E., Alling, V., Kosmach, D., Charkin, A., Semiletov, I.P., Dudarev, O.V., Shakhova, N., Roos, P., Eglinton, T.I., Andersson, A., Gustafsson, O., 2012. Activation of old carbon by erosion of coastal and subsea permafrost in Arctic Siberia. *Nature* 489 (7414), 137–140. <http://dx.doi.org/10.1038/nature11392>.
- Vonk, J.E., Mann, P.J., Davydov, S., Davydova, A., Spencer, R.G.M., Schade, J., Sobczak, W.V., Zimov, N., Zimov, S., Bulygina, E., Eglinton, T.I., Holmes, R.M., 2013a. High biolability of ancient permafrost carbon upon thaw. *Geophys. Res. Lett.* 40 (11), 2689–2693. <http://dx.doi.org/10.1002/grl.50348>.
- Vonk, J.E., Mann, P.J., Dowdy, K.L., Davydova, A., Davydov, S.P., Zimov, N., Spencer, R.G.M., Bulygina, E.B., Eglinton, T.I., Holmes, R.M., 2013b. Dissolved organic carbon loss from Yedoma permafrost amplified by ice wedge thaw. *Environ. Res. Lett.* 8 (3), 035023. <http://dx.doi.org/10.1088/1748-9326/8/3/035023>.
- Walter Anthony, K.M., Zimov, S.A., Grosse, G., Jones, M.C., Anthony, P.M., Chapin III, F.S., Finlay, J.C., Mack, M.C., Davydov, S., Frenzel, P., Frolking, S., 2014. A shift of thermokarst lakes from carbon sources to sinks during the Holocene epoch. *Nature* 511, 452–456. <http://dx.doi.org/10.1038/nature13560>.
- Walter, K.M., Edwards, M.E., Grosse, G., Zimov, S.A., Chapin, F.S., 2007. Thermokarst lakes as a source of atmospheric CH₄ during the last deglaciation. *Science* 318 (5850), 633–636. <http://dx.doi.org/10.1126/science.1142924>.
- Ward, C.P., Cory, R.M., 2015. Chemical composition of dissolved organic matter draining permafrost soils. *Geochim. Cosmochim. Acta* 167, 63–79. <http://dx.doi.org/10.1016/j.gca.2015.07.001>.
- Zimov, S.A., Davydov, S.P., Zimova, G.M., Davydova, A.I., Schuur, E.A.G., Dutta, K., Chapin, F.S., 2006. Permafrost carbon: stock and decomposability of a globally significant carbon pool. *Geophys. Res. Lett.* 33 (20), L20502. <http://dx.doi.org/10.1029/2006GL027484>.
- Zimov, S.A., Zimov, N.S., Tikhonov, A.N., Chapin Iii, F.S., 2012. Mammoth steppe: a high-productivity phenomenon. *Quat. Sci. Rev.* 57 (0), 26–45. <http://dx.doi.org/10.1016/j.quascirev.2012.10.005>.
- Zubrzycki, S., Kutzbach, L., Pfeiffer, E.M., 2014. Permafrost-affected soils and their carbon pools with a focus on the Russian Arctic. *Solid Earth* 5 (2), 595–609. <http://dx.doi.org/10.5194/se-5-595-2014>.